POLITECNICO DI TORINO

Master's degree in Biomedical Engineering

Master's thesis project

Electrodes based on Cytochromes and nanostructured oxides with variable crystalline structure for the detection of Cyclophosphamide

Supervisors

Professor Alberto Tagliaferro (PoliTo),

Professor Sandro Carrara (EPFL),

Dr. Mattia Bartoli (IIT).

Candidate

Sara Graziani

Academic year 2023/2024

Abstract

Within the huge family of sensors technology, electrochemical sensors allow the transduction of a chemical information to an electrical signal to precisely characterize complex chemical phenomena, such as redox reactions, or to quantify the concentration of a molecule in a solution. Nanostructured metal oxides, with spinel crystalline structure, are attractive for electroanalytical methodologies because they could improve the catalytic activity of the redox process of some molecules: they could have the ability to enhance the detection' sensibility. Therefore, the aim of this work is to study the electrochemical performance of nanostructured metal oxides (i.e. $ZnCr_2O_4$, $ZnFe_2O_4$ and $CuFe_2O_4$) in the detection of Cyclophosphamide, an anticancer drug, whose metabolism relies on Cytochrome P450.
The nanoparticles were synthesized by adopting the auto-combustion technique and they were morphologically and chemically characterized by scanning electron microscopy and Raman spectroscopy. Nanostructured powders were then used to tailor the surface of screen-printed carbon electrodes by drop casting technique with or without the addition of Cytochrome P450 in his two isoforms of 3A4 or 2B6. Drug detection was acquired in phosphate-buffered solutions. This thesis project aimed then to unveil the effect of electrode surface functionalization on the electrochemical behaviour of the drug, considering different crystal lattice of the nanoparticles. The analyses were carried out with drug concentrations between 250 µM and 1 mM, using cyclic voltammetry and differential pulsed voltammetry techniques.
The results of bare electrode and spinel nanomaterials functionalized electrodes are comparable, providing a maximum Faradic current peak of 0.18 ± 0.08 µA with a sensitivity of 0.09 ± 0.04 nA/µM, obtained by the linear calibration of the sensor. Surface functionalization only with enzymes leads to an increase in the maximum current peak and in the sensitivity by an order of magnitude. However, the best results are obtained with the synergetic coupling of nanostructured metal oxide and Cytochromes: the functionalization with $ZnCr_2O_4$ and Cytochrome P450 2B6 leads to a maximum of current peak of 9.24 ± 0.65 µA and a sensitivity of 6.90 ± 0.41 nA/µM. Instead, concerning the limit of detection, the best performance is with $ZnFe_2O_4$ and Cytochrome P450 3A4, with a value of 20.04 ± 0.98 µM.
From the analyses carried out so far, it is possible to conclude that the presence of nanostructured oxides has a catalytic action on the reductive process of the Cytochromes, and consequently of Cyclophosphamide, intensifying the signal that

is detected. Metal oxides with a normal spinel lattice with Cytochrome P450 2B6 seem to guarantee the best performance.
Promising results obtained suggest the necessity to conduct further research to optimize the application of these hybrid surface functionalizations in the field of biosensing.

Index

List of figures

List of tables

Chapter 1

Introduction

1.1 Electrochemical sensors

A sensor is a mechanical, electronic or chemical device that can convert physical data into signals, that provide qualitative and quantitative information about the process analysed. This technology is applied in chemical sectors, which include optical, magnetic, mass, thermal and electrochemical fields. In the latter sector, the sensors allow the transduction of a chemical information to an electrical signal, to precisely characterize complex chemical phenomena, such as redox reactions, or to quantify the concentration of a molecule in a solution. The electrical signal could be studied through a graphic representation [1]. Sensors are used in different fields including environmental monitoring, medical and pharmaceutical field, food industry, engineering and a wide range of commercial applications [2].
According to literature, electrochemical sensors, compared to other traditional instrumental analysis methods, such as mass spectrometry, fluorimetry, capillary electrophoresis, gas and liquid chromatography and nuclear magnetic resonance, present various advantages: they guarantee faster analysis times, lower equipment cost and the use of small volumes of samples [2]. They ensure a good selectivity and sensitivity: respectively, the ability to detect the target molecule compared to other substances present in the sample and the ability to provide a response with relatively large variations compared to the variations in the measured quantity. Moreover, they allow to obtain comparable or even better results than traditional analysis methods [1]. Wei et al. [3] propose an electrochemical sensor for oral cancer analysis based on the detection of interleukin-8 mRNA and interleukin-8 protein in saliva samples: the authors state that this sensor guarantees sensitivity and specificity comparable to the results obtain with enzyme-linked immunosorbent assay (ELISA) and polymerase chain reaction (PCR) assay, especially during the simultaneous detection of the two biomarkers.
Finally, electrochemical sensor is a versatile electrochemistry analysis technique because it provides a wide detection range and a good reliability in the investigation of numerous analytes [1]. They have been produced using various manufacturing methods, such as photolithography, screen printing and inkjet printing [4]. Screen printing technology consists of a layer-by-layer deposition of different inks upon a

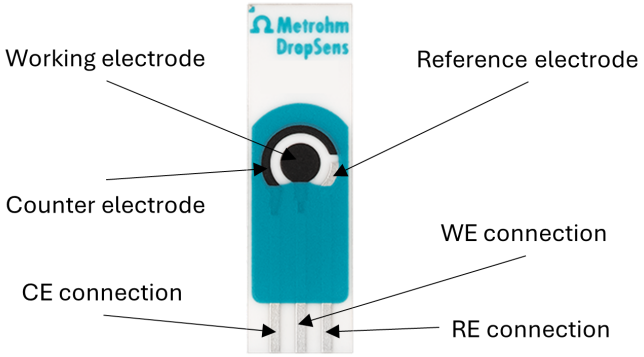

Figure 1: Screen-printed carbon electrode module [5].

solid substrate: a screen-printed electrode (SPE) is made of a chemically substrate, that should be made in an inert material to not interfere during the measurement, on which three electrodes called working electrode (WE), reference electrode (RE) and counter electrode (CE) are printed (Figure 1).
The production is based on some fundamental stages [4]:

- Selection of the screen or mesh to define the geometry and size of the SPE. The dimensions are around 3.5 x 1.0 x 0.05 cm and the WE area is around 0.10 cm^2.

- Selection and preparation of the inks. A wide range of materials can be employed and they must be chosen in relation to the process under analysis, because they have a big impact in the performance of the device. The most used materials for the WE are carbon, platinum or graphite; instead, the RE is usually made of $Ag/AgCl$ and the CE is made of the same material as the WE or it is an external platinum wire or rod [4].

- Selection and preparation of the substrate material; this aspect, of pivotal importance, presents several alternatives, which will be explored in the following sections.

- Printing, drying and curing [4].

The main advantages of this manufacturing technique are low production cost, precise control over electrode sizes, excellent uniformity of the surface, high reproducibility and scalability. Thanks to electrochemical sensors is possible to perform potentiometric, voltammetric, amperometric, conductometric, coulometric and impedimetric measurements. The potentiometric sensors present a surface

modification that catalyse the reaction with the target molecules: this process generate ions that are sensed. This methodology measures the potential difference between the WE, that monitors the accumulation of charge, and RE, under equilibrium conditions.
The voltammetric sensors record the current as a function of potential, that is variously applied either continuously, in the cyclic voltammetry technique, or step by step, in the differential pulse voltammetry technique, to obtain a voltammogram. The amperometric technique, instead, involves the measurement of the current at a fixed potential and the current is detected as a function of time [4]. Conductivity measurement, although it is not selective, it is a simple and versatile technology of electrochemical detection: the sensing cell consists of two inert electrodes placed one in front of the other in the flow channel of the target solution or wires placed across the flow path, parallel to it. They detect the conductivity of the solution and the change of it, due to the passage of diffuse ions to the electrode, is directly proportional to the concentration of the analyte in the sample [6].
Finally, coulometry is an absolute method in which the total charge consumed in the redox conversion of an analyte at an electrode surface is measured; the analyte in the sample volume is exhausted completely during the analysis. In contrast to most analytical methods, it determines, not the concentration, but the total amount of analyte, that is proportional to the electrical charge detected [7].
The great versatility of SPEs is in the wide range of ways in which the surface of the WE could be modified: this functionalization procedures can lead to an improvement in the detection performance, especially concerning the sensitivity and the limit of detection [4]. Carrara et al. [8] propose a biosensor with an electrode surface functionalization with enzyme and multi-wall carbon nanotubes that guarantees an enhanced sensitivity and decreased detection limit of some drugs, in comparison with bare surface and surface functionalized only with enzyme. A variety of materials, molecules and biomolecules are available for this purpose, like graphite powder, fullerene (C60), metal nanoparticles, nanomaterials, polymers, Nafion, cellulose acetate, biomolecules, enzymes, antibodies or the combination of them [9].

1.2 Sensing of molecules

The commonly used non-biological materials include diamond, graphite, metal nanoparticles, metal oxide nanoparticles, metal chalcogenides, metal–organic frame-

works, polymers, conducting polymers (CPs) or functionalized CPs, nanocomposite materials, carbon nanomaterials and carbon nanotubes. The specific lattice structure of nanomaterials has a remarkable impact on the electrochemical sensor application because they lead to a high active surface area per unit weight, high stability and conductivity. Moreover, they could lead to significant amplification of the analytical signal through altered electron-transfer kinetics. For example, thanks of their unique electrocatalytic properties, noble metal nanoparticles have captured the attention in research and gold is one of the most used noble metals in electrochemical sensor [1]. Sakthivel et al. [10] have designed a complex structure that combines gold and other materials for insulin detection; in particular, it is a sandwich structure made of Au nanoparticle (AuNP)-adhered to copper–zinc hollow porous carbon nanocubes ($Au@Cu_5Zn_8$/HPCNC) and AuNP-deposited nitrogen-doped holey graphene (NHG): they are used as a dual functional label and platform for sensing.

1.2.1 Spinel oxides materials

In this work the focus is on a specific class of materials: metal oxides with spinel crystalline structure. Their crystal lattice formula is $(A_{1-x}B_x)[A_xB_{2-x}]O_4$, where parentheses enclose cations in tetrahedral coordination, square brackets denote octahedral cation sites, while x, that have a value between 0 and 1, represents the degree of inversion which is meant either the fraction of tetrahedral sites occupied by cations 3^+ (B) or the fraction of octahedral sites occupied by cations 2^+ (A). In the crystal lattice, divalent and trivalent ions can occupy both octahedral and tetrahedral sites [11]. If x is 0, the structure is a normal spinel, i.e. zinc ferrite and zinc chromite; if x is 1, the structure is an inverse spinel, i.e. copper ferrite; if $0 < x < 1$, the structure is partially normal spinel or partially inverse spinel (Figure 2).

The degree of inversion in spinel oxides gives rise to important consequences in their properties: it influences the electrode surface heterogeneity and the catalytic activity of the material. Many reports show correlation between structural parameters, i.e. cations present in octahedral and tetrahedral sites, and the catalytic activity of spinel compounds: in oxide spinels, the catalytic activity is mainly due to octahedral cations [12]. Moreover, the physical, chemical and magnetic properties of metal spinel oxide nanostructures make them attractive for electroanalytical methodologies, improving the electroactive area and thus the sensitivity

and the limit of detection, compared to bare electrode surface [13]. They lead to a high surface-to-volume ratio, that facilitates subsequent functionalization of the surface, because it improves the binding with any organic molecules such as antibodies or enzymes [1].

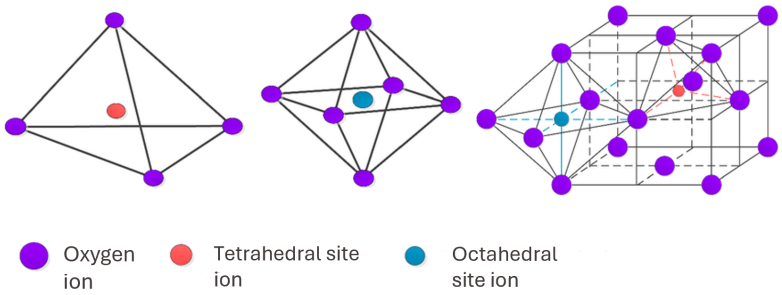

Figure 2: Example of spinel oxide crystal lattice [14].

1.2.2 Spinel oxides nanoparticles synthesis

There are many difficulties in manufacturing and characterisation of the spinel oxides nanoparticles, which encourage investment in finding increasingly reliable production methods [9],[15]. Moreover, the size and the shape of the nanoparticles affect the materials properties and their catalytic performances.
There are several methods of synthesis such as co-precipitation, micro-emulsion, thermal decomposition, sol-gel [16] and auto-combustion. It is important to know how to choose the method, based on the application you want to develop, as each of them has different advantages and disadvantages, as it is shown in Table 1. For example, considering the microemulsion method, the precursors are dissolved in water with micro drops in a first two-phase solution (aqueous/organic phases), whereas the basis is dissolved in micro-drops of a second two-phase solution; these two-phase solutions are mixed to promote the contact between micro-drops and, thus, the precipitation of the nanoparticles in a confined environment will take place. This technique guarantees a good size control, narrow size distribution and isolated particles; however, the yield is low and the crystallinity is poor.
The synthesis method applied in this work is auto-combustion because it is a simple, effective, single-step technique. The disadvantages are poor control in avoiding the aggregation of nanoparticles and low control of their size; it also ensures a high crystallinity structure, but it does not allow precise control over the growth of the crystallites [11].

Method	Advantages	Disadvantages
Co-precipitation	Soft conditions and easy modification surface	Large distribution of size, non controlled oxidation and low reproducibility
Micro-emulsions	Good size control, narrow size distribution and adjustable size and shape	Low yield, poor crystallinity and difficulties in washing surfactants
Thermal decomposition	Narrow size distribution, high crystallinity and isolated particles	High temperature and low yield
Auto-combustion	Simple, effective high crystallinity	Aggregation and low control of the size
Sol-gel	Soft conditions, narrow size distribution and high crystallinity	Long synthesis time

Table 1: Synthesis methods with their advantages and disadvantages [16].

1.3 Biosensing of molecules

In the field of electrochemical sensing, one of the main flaws of non-biologic nanomaterials is the lack of specificity towards the target molecules. On the contrary, the biomolecules guarantee high selectivity and specificity during the analysis process: therefore, in this section, the focus is on the surface functionalization of electrodes with biomaterials, evaluating their features.
In bio-electrochemical sensors, biomolecules, also called receptors, are classified into biocatalytic receptors, such as enzymes, and bio-affinity recognition elements, such as antibodies, aptamers and nucleic acid sequences. Other molecules widely used in biosensing are cells and tissues [1].

1.3.1 Enzyme-modified biosersors

The enzymes are globular proteins produced by living organisms and they are biological catalyst because they can speed up the rate of certain chemical reactions in cell metabolism. The interaction between the enzyme and the target molecule in the active site leads to the formation of enzyme–substrate complex [17].
One of many categories of enzymes is Cytochrome P450 (CYP P450). It is a metabolic enzyme present within the liver, in the hepatocytes, capable of catalysing around 75% of all drugs in use. CYPs are classified according to their amino acid sequence and the two isoforms used in this work are CYP P450 3A4 and CYP P450 2B6. Concerning their common features, their active-site area is quite rigid and it is surrounded by a more flexible complex binding areas: this guarantees some

conformational changes to allow the binding of different-size molecules. Moreover, they are characterized by a heme group in their active site that contain iron, which is crucial for the catalytic activity. Thanks to this group, CYPs behave like a metal as they can gain or lose electrons, catalysing substrate oxidations and reductions; this explain why they are used in the electrochemical analysis of redox processes [18].

The enzyme-based electrochemical sensors, also called enzymatic sensors, consist of an electrode functionalized superficially with specific enzymes, to analyse the analyte with good specificity and selectivity [1]. The higher the affinity between the enzyme and the target molecule, the better the detection performance will be. However, enzymes are fragile molecules that require suitable environmental conditions to maintain their stability and activity: free enzymes are easily inactivated and reusing them is difficult. Enzymatic immobilization on nanomaterials or nanoparticles is expected to solve these problems [19].

1.4 Hybrid biosensors

The simultaneous presence of biomolecules and non-biological materials is the distinctive feature of the category of sensors called hybrid electrochemical biosensors. They combine organic with inorganic building blocks and the total device presents physical and chemical characteristic that are distinct from the specific properties of the components alone. This partnership can work as signal amplifiers and as a catalyst of the electrochemical reaction of interest.

As shown in Figure 3, the main biological materials used in these sensors, such as proteins, antibodies, nucleic acid and microorganisms, are combine with non-biological materials, like silicon nanomaterials, polymers and quantum dots [20]. These materials have been combined in many ways according to the purposes of the final device; in this regard, Cajigas et al. [21] have developed a nano-bioconjugate sensor based on gold nanoparticles linked to single-strand DNA for the amplification of the electrochemical signal of a Zika virus genetic material-based bioassay, with high sensitivity.

If the biomolecule used is an enzyme, it is important to underline that the electron transfer between the protein and the electrode depends mostly on the technique used for the biological molecule immobilization. The functionalization technique influences the orientation and the conformational geometry of the molecule over the electrode. The strategies of receptor immobilization are classified into two cat-

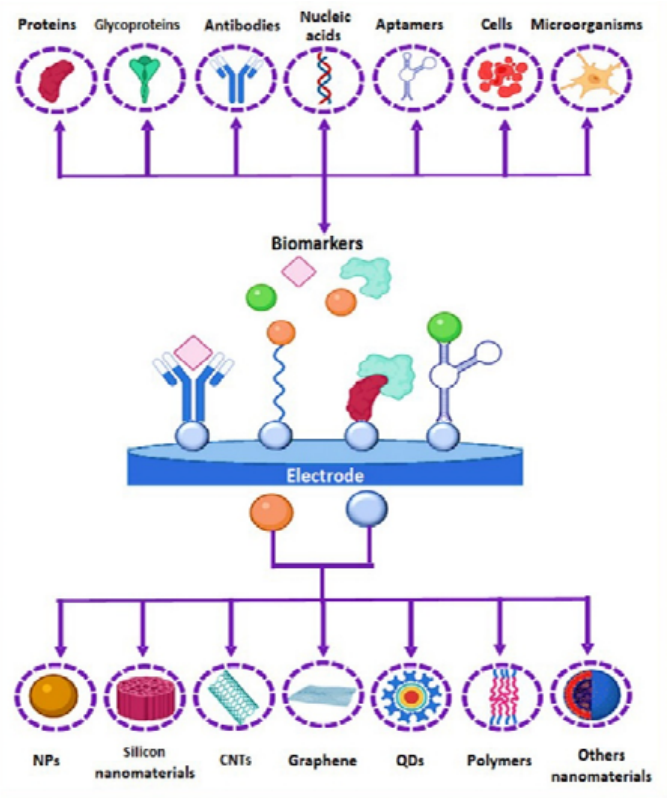

Figure 3: Scheme of electrochemical hybrid biosensors based on organic and non-organic molecules [20].

egories: non-covalent, such as adsorption, entrapment, or affinity, and covalent or cross-linking: Table 2 shows a summary of their advantages and disadvantages [1]. An application, concerning the covalent immobilization strategy, is the research carried out by Bahrami et al.[22]: glutaraldehyde pre-activated super paramagnetic iron oxide nanoparticles are used for the covalent immobilization of CYP P450 BM3 from Bacillus megaterium, to study the effect of glutaraldehyde as a coupling agent on immobilized BM3 activity. This work has demonstrated that this type of functionalisation allows better results than the free enzyme condition. It is an effective, but complex immobilization technique; alternatively, drop casting technique, a simpler and faster methodology, allows to obtain good results [23].

1.5 Cyclophosphamide sensing

Thanks to hybrid functionalized sensors, described in section 1.4, it is possible to detect and characterize different types of molecules, including drugs; in this work the focus is on the detection of the Cyclophosphamide (CP), shown in Figure 4. It is an anticancer chemotherapy drug with the ability to add an alkyl group to

Strategy	Type of binding	Advantages	Disadvantages
Adsorption - drop casting	Weak bonds	Easy and simple	Detachment and risk of non-specific interaction
Covalent	Chemical	Stable, short time reaction and preserving the receptor activity	Non-reversible
Entrapment	Physical / mechanical	No chemical reaction and possibility to immobilize several types of receptors within the same surface	Requiring high concentration of the materials
Affinity	Natural binding	Easy to control and orient the attachment	Requiring specifc groups on the receptor (e.g. avidin–biotin interaction)

Table 2: Strategies for receptors immobilization with their advantages and disadvantages.

the guanine bases of DNA: this alkylating action modifies the DNA sequence and prevents its proper duplication during the cell reproduction. In this way, the proliferative capacity of the cancer cell is compromised.

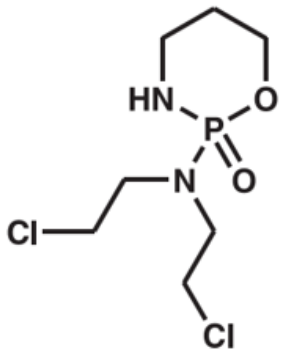

Figure 4: Chemical structure of Cyclophosphamide, $C_7H_{15}Cl_2N_2O_2P \cdot H_2O$ [24].

Cyclophosphamide is a derivative of mustard gas and the first alkylating agent was identified in one of its derivatives, which became a form of chemotherapy effective. It is approved by the Food and Drug Administration for the treatment, for example, of Hodgkin's lymphoma, Burkitt's lymphoma, different types of leukaemia, neuroblastoma, breast, testicular, endometrial and lung cancers [25]. It is activated within the liver thanks to the action of CYPs P450 which trigger its reductive process. In physiological conditions and in an aerobic environment, it is characterized by an irreversible reduction process [24], [26].

To monitor the concentration of the drug within the body fluids, traditional analysis techniques, such as flame ionization gas chromatography or chromatography-

mass spectrometry, can be applied. However, these methods are highly complicated, expensive and require specialized personnel [27]. Alternatively, it is possible to use electrochemical sensors, as done in the study carried out by Sinha et al. [28], where the differential pulse cathodic adsorptive stripping voltammetry was optimized, using a glassy carbon electrode, for determination of Cyclophosphamide in human urine as biological sample.

1.6 Project aim

This thesis project aimed to unveil the effect of electrode surface functionalization, with nanostructured metal oxides (i.e. zinc chromite, zinc ferrite and copper ferrite) and CYP P450 in his two isoforms of 3A4 or 2B6, on the electrochemical behaviour of Cyclophosphamide.

The focus is to study the electrochemical performance of nanostructured spinel oxides in a synergetic coupling with CYP P450, to investigate both the performance of the enzymes and the properties of the crystal lattice of the nanoparticles, to understand if they can lead an enhancement in the sensing. Thanks to the drop casting of the analyte solution on the SPE functionalized surface, the analyses were carried out with drug concentrations between 250 µM and 1 mM, using cyclic voltammetry and differential pulsed voltammetry techniques. The performances of the sensing electrode are quantified through its sensitivity, limit of detection and maximum current peaks. The goal is to determine the surface functionalization that exhibit the best performance, thereby paving the way for further applications in the field of sensing and biosensing.

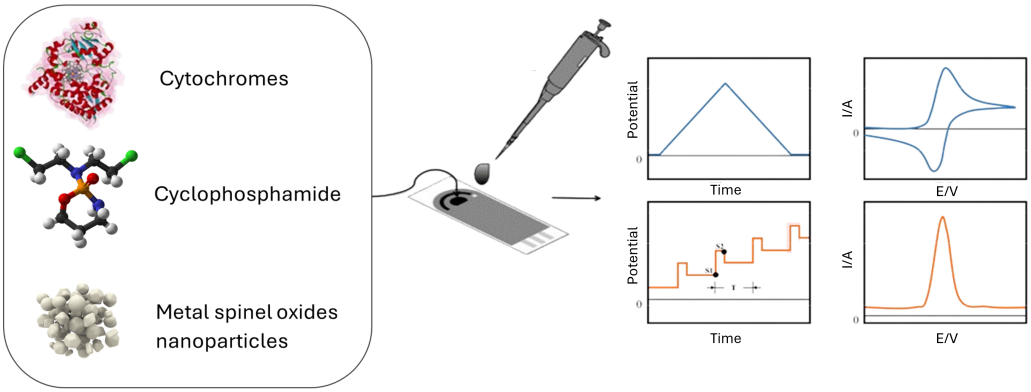

Figure 5: Project summary flow chart.

Chapter 2

Theoretical background

To understand the phenomena that occur at the interface between solution and electrode during the analysis, it is necessary to know the chemical, physical and mathematical theorical backgrounds. In this chapter the main theoretical aspects applied in the analysis are described and summarized.

2.1 Theory of electrochemistry

Electrochemistry is based on the relationship between chemical changes and flows of electrons: the pivotal process to describe this phenomenon is the redox reaction. The term redox, indeed, summarizes the oxidation-reduction process, characterized by an exchange of one or more electrons between two interacting elements, one acting as an electron donor and the other acting as an electron acceptor. An example, considering simple and inorganic species, is the following reaction:

$$Zn + Cu^{2+} \rightarrow Cu + Zn^{2+}, \tag{1}$$

in which Cu^{2+}, the acceptor, is reduced by acquiring two electrons from Zn, the donor, which then oxidizes. This happens because the lowest unoccupied molecular orbital (LUMO) of Cu^{2+} is at a lower energy than the electron in the highest occupied molecular orbital (HOMO) of Zn. The transfer of an electron between the two molecules in a liquid solution is a homogeneous electron transfer and the driving force for the reaction is the difference in energy levels. This phenomenon is schematized in Figure 6, where the blue horizontal lines represent the HOMO and LUMO energy levels, of Zn and Cu^{2+} respectively.
Instead, between a liquid solution and a solid surface of the electrode, the redox process is characterized by a heterogeneous electron transfer. Here, the driving force for the reaction is the energy difference between the LUMO of the molecule and the energy level of the electrode, that is modulate using an external power source, such as a potentiostat [29]. The electronic exchange generates a current that can be quantified (Figure 6).
In the case of SPE, when you apply a tuned potential, the electrochemical event of interest occurs on the WE, as a function of the RE potential. If the redox process of the analyte takes place, the current begins to flow and it is recorded as electrons

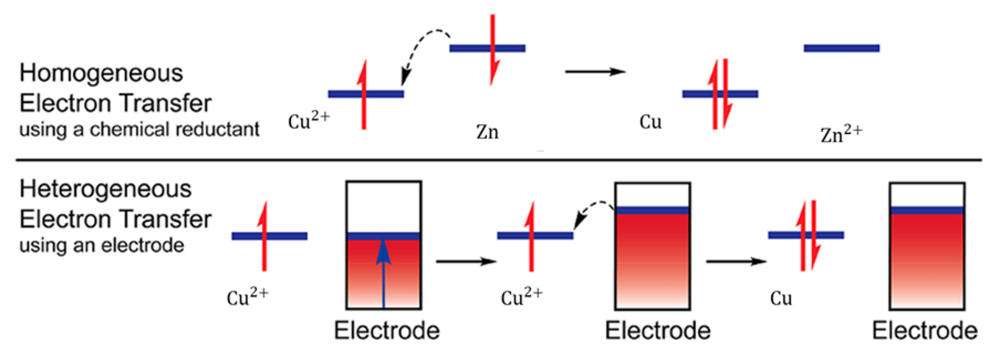

Figure 6: Scheme of an homogeneous and heterogeneous electron transfer [29].

flow between the WE and CE, whose purpose is to complete the electrical circuit [29]. To explain a redox process involving organic systems, such as enzymes, it is not correct to assume net charge transfers between atoms, so these reactions are described in terms of interactions between electrophiles and nucleophiles. Traditionally, in the organic field, redox models of oxygen or hydrogen transfer are used [30]. As an example, two simple reaction are shown.

$$C + O_2 \rightarrow CO_2, \tag{2}$$

$$H_2 + Cl_2 \rightarrow 2HCl. \tag{3}$$

The discussion becomes further complicated when the redox process involves organic and inorganic molecules at the same time. The case in question is the Cyclophosphamide reduction process mediated by CYP P450 and spinel oxide. The electrode transfer, which starts from the surface of the carbon electrode, is thermodynamically enhanced by the chemical structure and crystal lattice of the nanoparticles; then, the electrodes, thanks to the heme group of the enzyme and in presence of oxygen, reach the target substrate, i.e. the drug, and allow its reduction [18].

2.2 Nernst equation

The relationship between the potential applied to the electrode and the concentration of reactive species in solution is described by the Nernst equation: it relates the electromotive force of an electrochemical cell, called electrode potential, E, to the solution concentrations and temperature. Nernst equation describes a condition of electrochemical equilibrium:

$$E = E^0 + \frac{RT}{nF} ln \left(\frac{Ox}{Red} \right) \tag{4}$$

where E^0 is the standard cell potential, F is the Faraday constant, $F = 96485$ $Cmol^{-1}$, n is the number of electrons transferred in mol, $R = 8.314$ $Jmol^{-1}K^{-1}$ is the universal gas constant, T is the temperature in Kelvin and *(Ox)* and *(Red)* are the activities of the oxidized and reduced analyte. In practical application of the equation, the activities are replaced with their concentrations, c_O and c_R, the standard potential E^0 with the formal potential $E^{0'}$ and n is set equal to one.

$$E = E^{0'} + \frac{RT}{nF} ln \left(\frac{c_O}{c_R}\right) \tag{5}$$

Therefore, in standard conditions, such as ions unitary concentration, the cell potential is $E = E^{0'}$, because the second term of Equation 5 becomes zero [31]. The Nernst equation leads to understand how a system will respond to a change of concentration of species in solution or a change in the electrode potential [29].

2.3 Irreversibility of the redox process

A heterogeneous reversible redox reaction, in electrochemistry, is described by the general Equation 6 and Equation 7:

$$Ox + ne^- \rightarrow Red \tag{6}$$

$$Red \rightarrow Ox + ne^- \tag{7}$$

where Ox is the oxidized form of a solution species, Red is the reduced form of a solution species and n is the stoichiometric number of electrons in the process.
The standard heterogeneous rate constant, k_s, describes the electron transfer rate and it is determined by the type and complexity of the molecules undergoing electron transfer and the molecular rearrangements that may occur following electron transfer. Reversibility requires that the electron transfer kinetics are fast enough to maintain c_O and c_R near the electrode surface at the values required by the Nernst equation, so both the reduction and oxidation processes take place, as they are thermodynamically favorable. Hence, reversibility depends also on the scan rate of the potential, v, applied during the voltammetry analysis: if the ratio of k_s/v is sufficiently small that Nernstian concentrations cannot be maintained, then the process is said to be quasi-reversible or irreversible. In this condition, there is a high barrier to electron transfer and the reactions of electron transfer are slower compared to mass transport: more negative or positive potentials are required to observe reduction or oxidation processes.

2.4 Mass transport kinetics

Electrochemical kinetics describes the rates of the reactions that take place at the interface between the liquid solution and the solid surface of the electrode: these are therefore heterogeneous reactions that occur thanks to a mass transport of the reacting molecule from the bulk of the solution to the surface of the electrode and the consequent removal of the reaction products. The motions that characterize an electrolyte solution are

1. diffusive, due to a concentration gradient;
2. migratory, induced by an electric potential gradient;
3. convective, governed by gradients of temperature, density or pressure.

The analysis conditions applied in this work allow to simplify the treatment, neglecting the convective motion since the solution is not subjected to agitation and the temperature is kept constant. Moreover, the electric potential gradient can be neglected because the drug detection has been acquired in phosphate-buffered (PB) solutions, which is an inert electrolyte. It does not affect the reaction under analysis and it is in higher concentration than that of the drug. Mass transport kinetics inside the solution is therefore dominated by a diffusive motion.

2.5 Fick's laws

As mention before, the redox process is influenced by the motion of the drug inside the solution. The diffusive motion of neutral particles is mathematically described by the Fick's laws: the first law, Equation 8, describes the diffusive flux J related to the concentration gradient.

$$-J(x,t) = D\frac{\partial C(x,t)}{\partial x}, \tag{8}$$

where D is the diffusion coefficient of the diffusing species, $\mathbf{C}$ is the species concentration and x is the distance from the electrode surface.
Moreover, the second law, Equation 9, predicts the diffusion process with respect to time and it allows to obtain information about the trend of the analyte concentration with respect to the distance from the electrode surface and the electrolysis time, t, [32].

$$\frac{\partial C(x,t)}{\partial t} = D\frac{\partial^2 C(x,t)}{\partial^2 x}. \tag{9}$$

The current generated during a redox process is proportional to the flux, J, and to the electrode surface area, A; it is described by the Equation 10:

$$i = FAJ. \tag{10}$$

2.6 Theory and operation of cyclic voltammetry

To investigate the reduction and oxidation processes of molecular species Cyclic voltammetry (CV) is commonly employed: it is an electrochemical technique based on the application of a triangular shape potential between the working electrode and the reference electrode. According to the Nernst equation (5), when the potential is scanned during the voltammetry analysis, the concentration of the species, reagents or products, in solution in the environment near the electrode changes over time: in fact, the change in potential generates a diffusive motion, from the bulk to the electrode surface and vice versa, of the reactive molecules within the solution. This process is described by the formation of a current, Equation 10, and current peaks, within the voltammogram, whose intensity is proportional to the concentration of the species in the solution that is oxidizing or reducing, at a specific potential value.

In Figure 7, two distinct current peaks are distinguishable, one associated with the reduction and the other with the oxidation process. On the other hand, if it is an irreversible process, the graph generally has only one peak, which potential corresponds to the oxidative or reductive reaction of the analyte. The higher the concentration of molecules involved in the redox process, the greater is the electron exchange between solution and electrode surface.

The most important parameters are start potential (V), upper vertex potential (V), lower vertex potential (V) of the triangular shape and scan rate (mV/s). It influences the analyte diffusivity near the electrode surface: faster scan rates enhance diffusion motion and higher current peaks are observed.

At the end of the analysis the result is a voltammogram or cyclic voltammogram where the x-axis represents the applied potential (E), while the y-axis is the resulting current (i) flowed between WE and CE, as shown in Figure 7 [29]. The study of this graph is a means to understand the mechanisms of reactions and to calculate the kinetics of some processes.

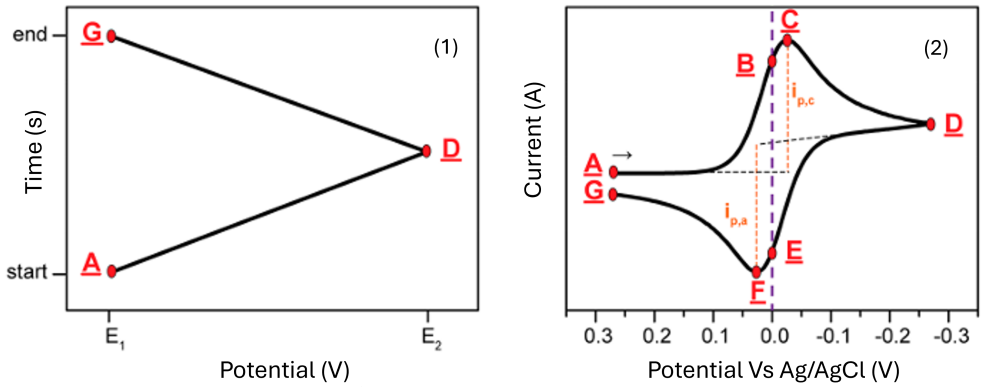

Figure 7: (1) Schematic diagram of a CV waveform. E_1 is the start and final potential, E_2 is the upper vertex potential. (2) Voltammogram of a reversible process. i_{pc} is the reduction current peak and i_{pa} is the oxidation current peak [29].

2.7 Theory and operation of differential pulse voltammetry

Differential pulse voltammetry (DPV) is a step by step technique where the potential is stepped to a slightly higher potential on each step: small amplitude pulses are superimposed following a linear ramp and current is measured before the application of the pulse (*I(1)*) and at the end of each pulse (*I(2)*), as shown in Figure 8.

In the voltammogram the x-axis represents the applied potential (E), while the y-axis is the resulting current (i) from the difference of the currents between each pulse (*I(2)-I(1)*). The most important parameters are start potential, stop potential, step and modulation amplitude.

The major advantage of DPV is the reduction of the background current due to the direct current ramp, that leads to a high sensitivity. This happens because the sampling periods are selected to allow sufficient time for non-Faradaic current to decay, so that only current arising from Faradaic reactions is reported. DPV is often used to discriminate analytes that have similar oxidation potentials or small redox peaks, because it enhances the amplitude of voltammetric peaks, in comparison with CV. Moreover, DPV leads to a higher sensitivity to better distinguish small changes in the maximum of the peak current, corresponding to the redox process of the analyte [33], [34].

In this analysis, the applied potential is unidirectional, so, based on the redox half-process to be studied, it is necessary to choose the appropriate potential di-

rection. In this work, since the focus is on the reductive process of the enzyme, and therefore of the drug, a decreasing potential has been applied, from higher to lower values.
In addition, the correspondence between CV voltammogram and DPV voltammogram is always valid, since they are two different techniques, but they describe the same reaction in progress.

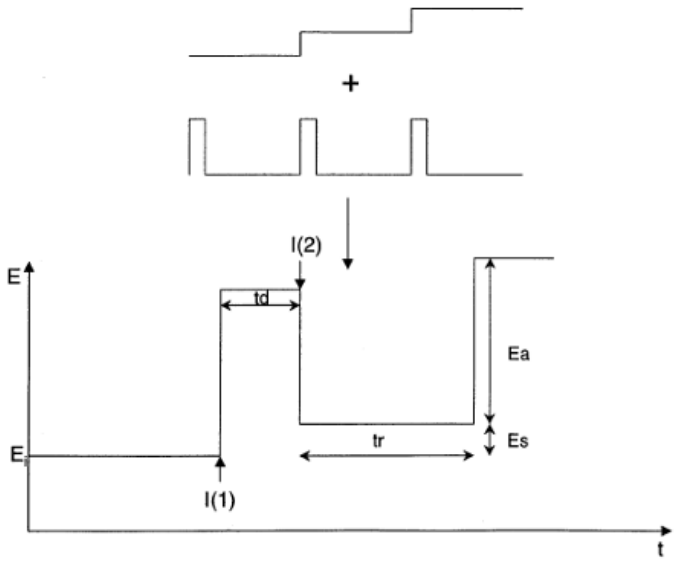

Figure 8: Schematic diagram of a DPV waveform. E_i is the initial potential, *I(1)* and *I(2)* are the times at which the current is sample, E_a is the potential amplitude of the applied pulse, E_s is the size of the step, t_d is the duration of the pulse and t_r is the time between each pulse [34].

2.8 Limit of detection

When the voltammetry analysis is carried out with different concentrations of the analyte in the solution, it is possible to derive a calibration curve of the sensor; the slope of this curve coincides with the sensitivity of the sensor, that is a pivotal parameter for quantifying the performance of the analysis. The greater the sensitivity of the sensor, the greater the possibility of distinguishing small variations in concentration of the analyte in the solution.
Sensitivity is also involved in study of the limit of detection (LoD), that is the smallest measure that can be detected, with reasonable certainty, for a given analytical procedure and it is expressed as a concentration or quantity [35].

The Equation 11 is used to calculate the lowest detectable concentration.

$$LoD = \frac{ts}{r} \tag{11}$$

Here, r is the sensitivity, t is Student's constant which takes a value of 3 and s is the standard deviation of the measurements in the absence of analyte, i.e. the empty samples. It is important to note that (i) the errors are assumed to have a Gaussian distribution and (ii) the error distributions of empty samples and low-concentration measurements have the same amplitude [36].

Chapter 3

Materials and methods

3.1 Nanomaterials synthesis

The three types of spinel oxide nanoparticles, zinc ferrite ($ZnFe_2O_4$), zinc chromite ($ZnCr_2O_4$) and copper ferrite ($CuFe_2O_4$), were synthesised via the auto-combustion technique, at the Carbon group laboratories at Politecnico of Torino.
Zinc (II) nitrate hexahydrate ($Zn(NO_3)_2 \cdot 6H_2O$), iron (III) nitrate nonahydrate ($Fe(NO_3)_3 \cdot 9H_2O$), copper (II) nitrate trihydrate ($Cu(NO_3)_2 \cdot 3H_2O$), chromium (III) nitrate nonahydrate ($Cr(NO_3)_3 \cdot 9H_2O$) and zinc (II) nitrate monohydrate ($Zn(NO_3)_2 \cdot H_2O$) powders, as oxidizing agents, and urea powder (CH_4N_2O), as reducing agent, were mixed and homogenized with the use of a mortar inside a crucible. All the powders were provided by Sigma-Aldrich. The weight of each component, measured with a microbalance, was evaluated in stochiometric ratio to obtain 1g of metal oxide at the end of the process; the precise values are shown in Table 4. Afterwards, the crucible was put in a graphite reactor and it was placed inside a furnace; the materials were heated from room temperature to 600 °C, that was kept constant for 1 hour. Then, the final products, shown in Figure 9, were cooled under atmospheric conditions and the powder of metal oxides were collected; the yield of this process is shown in Table 3.

Metal oxide nanoparticles	**Yield**
Zinc ferrite	85%
Copper ferrite	88%
Zinc chromite	70%

Table 3: Nanoparticles synthesis yield.

	$ZnFe_2O_4$ (g)	$CuFe_2O_4$ (g)	$ZnCr_2O_4$ (g)
$Zn(NO_3)_2 \cdot H_2O$	1.234	–	–
$Fe(NO_3)_3 \cdot 9H_2O$	3.351	3.378	–
$Cu(NO_3)_2 \cdot 3H_2O$	–	1.010	–
$Cr(NO_3)_3 \cdot 9H_2O$	–	–	3.429
$Zn(NO_3)_2 \cdot 6H_2O$	–	–	1.275
CH_4N_2O	0.249	0.251	0.257

Table 4: Precursors weight for nanoparticles synthesis. Measurement uncertainty equal to 10^{-3}.

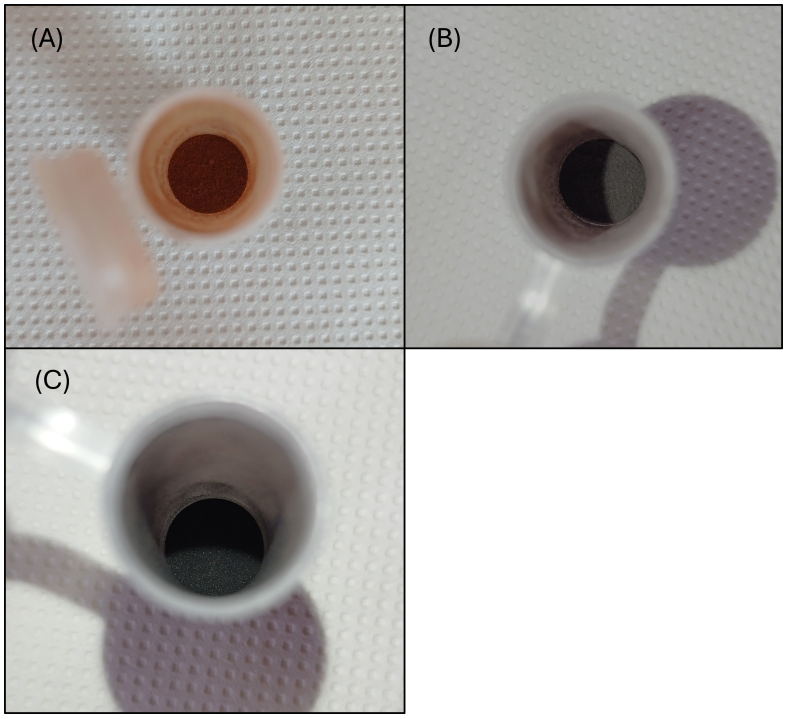

Figure 9: Metal spinel oxides powders. (A) $ZnFe_2O_4$ nanoparticles. (B) $ZnCr_2O_4$ nanoparticles. (C) $CuFe_2O_4$ nanoparticles.

3.2 Materials characterization

3.2.1 Raman spectroscopy

Raman spectroscopy is a non-destructive technique for the surface characterisation, which provides detailed information about chemical structure, phase, crystallinity, environmental features and molecular interactions. It is based on the impact of a high intensity laser light source over the material. The interaction between the light and the material molecules generate a scattering signal of light with a different wavelength from the source: this depends on the chemical structure of the analyte.
The result of the analysis is a Raman spectrum features several peaks with different intensity and wavelength position, for each molecular bond vibration, that represent a sort of fingerprint of the analyte [37]. The samples are here characterised using Renishaw, inVia Raman Microscope, with a laser wavelength of 785 nm (IR light) and a power of 0.5 mW.

3.2.2 Field emission scanning electron microscopy

Field emission scanning electron microscopy (FESEM) is a technique used for the characterization of materials that provides information about surface structure, morphology, composition and defects, even at a depth of a few micrometres.
The images, with a resolution of up to 1 nm, are obtained by scanning a beam of high-energy electrons on the surface of the sample. The electrons beam, that penetrates the surface, interacts with its atoms and generates secondary and backscattered electrons that are collected and processed to obtain images of the sample surface. In addition, the interaction of the electron beam with the sample emits X-rays with a specific energy that can be detected and identified to determine the chemical composition of the tested material [38]. To increase the conductivity of the surface and improve the sharpness and quality of the image, before the analysis, the surface is subjected to a sputtering treatment with platinum. In this work, SEM Zeiss Supra 40 is used to carry out the characterization. The images are obtained using secondary electrons and the energy of the electron beam is fixed at 5 keV.

3.3 Cyclophosphamide solution

The drug under investigation is Cyclophosphamide CRS and it was provided by European Pharmacopoeia Reference Standard. To prepare 1.0 mM solution, it was necessary to combine 2.9 mg of the drug powder in 10.4 mL of 0.1 M PB solution, that was used as electrolyte and it had a pH of 7.4 at 25 °C. Cyclophosphamide solutions with lower concentrations were obtained by diluting with PB the 1.0 mM solution: all the specific quantities of PB and drug used are shown in Table 5. The solutions were stored at a constant temperature of 4 °C.

Solution concentration (µM)	**CP 1.0 mM volume (mL)**	**PB 0.1 M volume (mL)**
250	0.30	0.90
500	0.60	0.60
650	0.78	0.42
800	0.96	0.24

Table 5: Volumes of 0.1 M PB and 1 mM Cyclophosphamide (CP) solutions used to obtain 1.2 mL of CP solutions at the desired concentrations.

3.4 Nanomaterials solution

To prepare a homogeneous solutions with zinc ferrite, zinc chromite and copper ferrite nanoparticles, it was necessary to combine 12 mg of metal oxides powders in 4 mL of distilled water (3:1 ratio). Afterwards, the suspensions were kept in an ultrasonic bath for 15 minutes until the solutions became homogeneous. They were stored at room temperature, under controlled atmosphere [39].

3.5 Electrode functionalization

Metrohm 11L screen-printed carbon electrodes (SPCE), from Metrohm DropSens, were used to carry out the analyses; the electrode sizes are 3.4 x 1.0 x 0.05 cm and the WE area is 0.11 cm^2. Moreover, it has the WE and the CE made of carbon and the RE made of $Ag/AgCl$ [5].
For the electrode surface functionalization, drop-casting technique was applied

by spreading 5 µL of metal oxides suspension over the WE surface. To allow the stabilization of the nanoparticles on the surface, it was important to let the functionalized surface dry overnight at room temperature and the electrodes were stored under atmospheric conditions [39]. Afterwards, it was possible to obtain the surface functionalization with human enzymes through a simple drop-casting technique of 5 µL of CYP P450 3A4 or 2B6 solution over the WE; the concentration of the enzyme solutions was 0.5 nM and they were provided by Corning $Supersomes^{TM}$. To allow the binding between the biological molecule and the nanoparticles, it was necessary to let the surface dry overnight at 4 °C [23].

3.6 Cyclic voltammetry and Differential pulse voltammetry measurements

Both the preparation of the solutions, the surface functionalization of the electrodes and the voltammetry analysis were performed under the fume hood and they were carried out at the Bio/CMOS Interfaces group laboratories at École Polytechnique Fédérale of Lausanne, in Neuchâtel.
AUT302N.MBA.S potentiostat, provided by Autolab Metrohm, was used for the electrochemical measurements. The equipment was connected to a laptop to carry out the data acquisition thanks to Nova 2.1.7 software; subsequently, the graphs were processed through OriginLab 2024 software.
Thanks to the potentiostat, it was possible to perform CV analysis to get a general idea of the reactions process, during the growth and decrease of the potential; moreover, it was possible to perform DPV measurements. According to the protocol, the analyses consist of a set of three electrodes at a time, to ensure the statistical significance of the results.
It was important to wash the surface of the bare electrode with deionized water, let it air dry and then perform the surface functionalization with metal oxides nanoparticles, enzymes or both. To clean and stabilize the electrode surface the first test was with PB, through the drop casting of 100 µl of electrolyte solution over the electrode surface; it represents also a reference for subsequent results comparisons. Afterwards, the protocol consists in three cycles of CV and immediately after DPV detection, in the same electrode, without changing the solution. We proceed with the analyses in this order because it has been observed that the first CV analysis helps the enzyme to take on the right conformation: this guarantees greater reduction current peaks, compared to those obtained by carrying

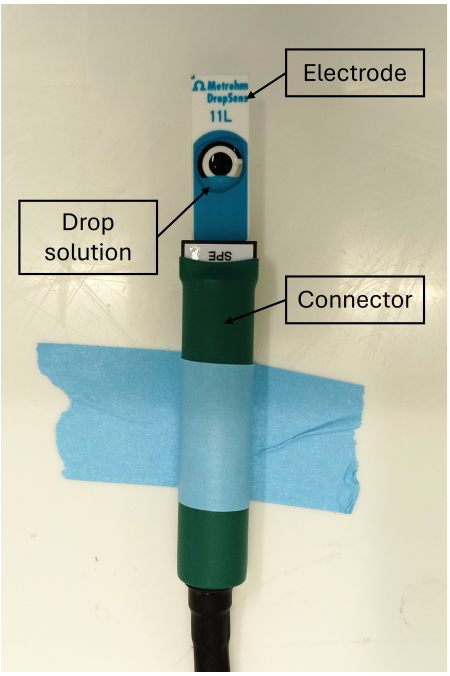

Figure 10: Example of electrode under analysis. The connector allows the transmission of the potential from the potentiostat to the electrode and the consequent detection of the signal.

out only a DPV analysis. The next operation was the drop casting of 100 µl of Cyclophosphamide solution over the electrode surface, starting from the lowest concentration, 250 µM, and then increase, in steps of 150 µM, until 1 mM, and perform a CV and DPV detection; between each analysis, every time you change the solution, wash the surface of the electrode with deionized water and let it air dry. The parameters used to carry out the analyses are shown in Table 6.
For the most comprehensive data comparison possible, the protocol was applied with different types of electrodes functionalization. First, the performance of bare electrode was analysed, followed by the tests of $ZnFe_2O_4$, $ZnCr_2O_4$ and $CuFe_2O_4$ nanomaterials functionalized electrodes. Subsequently, the analyses were carried out with the surface functionalization with CYP P450 2B6 and CYP P450 3A4. Finally, the behaviour of the three types of spinel metal oxides with the enzymes was studied. The Table 7 presents a summary of all the conditions considered.
As mentioned before, all the analyses were carried out considering the concentrations of Cyclophosphamide 250 µM, 500 µM, 650 µM, 800 µM and 1 mM: since five different results were obtained for each type of surface functionalization, it was possible to derive the calibration curves, where the maximum current peak average value of three electrodes, for each concentration, was evaluated.

CV parameters		**DPV parameters**	
Upper vertex potential (V)	0.4	Start potential (V)	0.4
Start potential (V)	-0.6	Stop potential (V)	-0.6
Lower vertex potential (V)	-0.6	Step (V)	-0.005
Scan rate (mV/s)	20	Modulation amplitude (V)	0.1
Number of scans	3	Number of scans	3

Table 6: Cyclic voltammetry and Differential pulse voltammetry parameters.

Electrode surface functionalization
Bare
$ZnFe_2O_4$ NPs
$ZnCr_2O_4$ NPs
$CuFe_2O_4$ NPs
CYP P450 2B6
CYP P450 3A4
$ZnFe_2O_4$ NPs with CYP P450 2B6
$ZnCr_2O_4$ NPs with CYP P450 2B6
$CuFe_2O_4$ NPs with CYP P450 2B6
$ZnFe_2O_4$ NPs with CYP P450 3A4
$ZnCr_2O_4$ NPs with CYP P450 3A4
$CuFe_2O_4$ NPs with CYP P450 3A4

Table 7: Summary of the electrode surface functionalizations analysed.

Chapter 4

Results and discussion

4.1 Materials characterization

Through Raman spectroscopy and Field emission scanning electron microscopy, the chemical and morphological characteristics of the synthesized powders are evaluated.

4.1.1 Raman spectroscopy

The spinel oxide nanoparticles powders were subjected to a Raman spectroscopy analysis to reveal their chemical characteristics and to validate the synthesis process applied. The results are shown in Figure 11, and they are compared with the Raman spectra of the same materials, present in literature in Figure 12.
$CuFe_2O_4$ exhibits six characteristic peaks: three T_{2g} bands, one E_g band, one A_g band and the peak occurred at 410 cm^{-1} indicates the presence of Fe_2O_3 in the material. $ZnFe_2O_4$, on the other hand, has five characteristic peaks: three T_{2g} bands, one E_g band and one A_g band. These results are confirmed through the comparison with the data in the literature [40], [11]. Finally, $ZnCr_2O_4$ presents four characteristic peaks: two F_{2g} bands, one E_g band and one A_g band. There is only a partial correspondence with the Raman spectra found in the literature. The reason for this discrepancy is that the reference information derives from analyses carried out at a different wavelength and laser power, compared to those performed in this work [41]. In this project the analyzes were carried out at a higher wavelength, that results in a variation of the intensity of the Raman signal with difficult identification of some peaks. Despite this, the spectrograms obtained allow to positively evaluate the powders synthesis process.

4.1.2 Field emission scanning electron microscopy

The FESEM analysis, carried out on the three metal spinels, aims to evaluate the morphology, size and shape of the nanoparticles. These characteristics are useful to validate the powder synthesis process: it is important, indeed, that the size dispersion of the nanoparticles is small, their shape is homogeneous and there is no agglomerate formation. Through the analysis of Figure 13, Figure 14 and

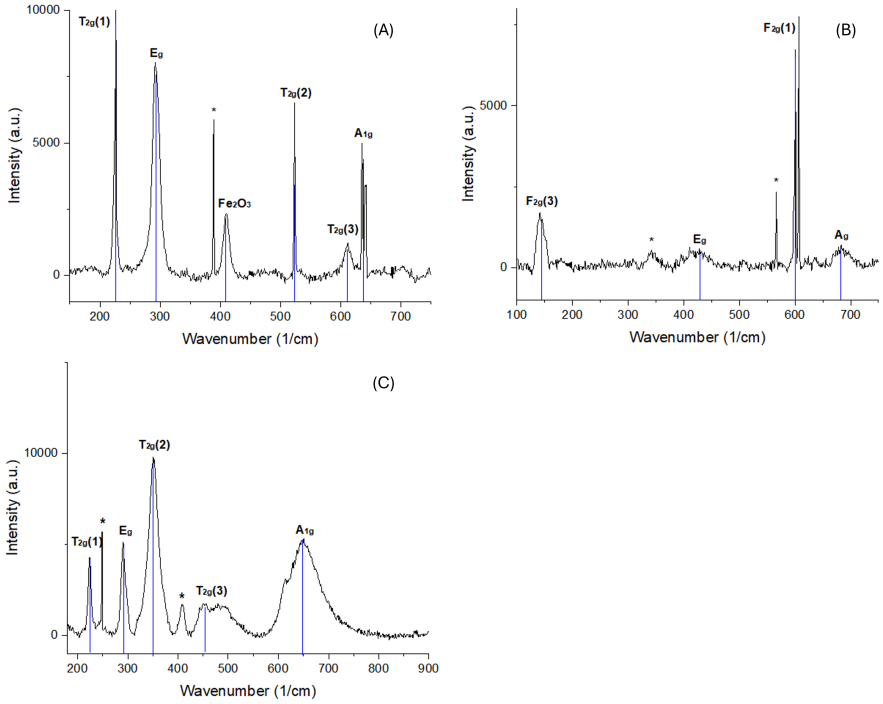

Figure 11: Raman spectra of the synthesized nanoparticles, * indicates an unknown Raman band. (A) $CuFe_2O_4$ Raman spectra. (B) $ZnCr_2O_4$ Raman spectra. (C) $ZnFe_2O_4$ Raman spectra.

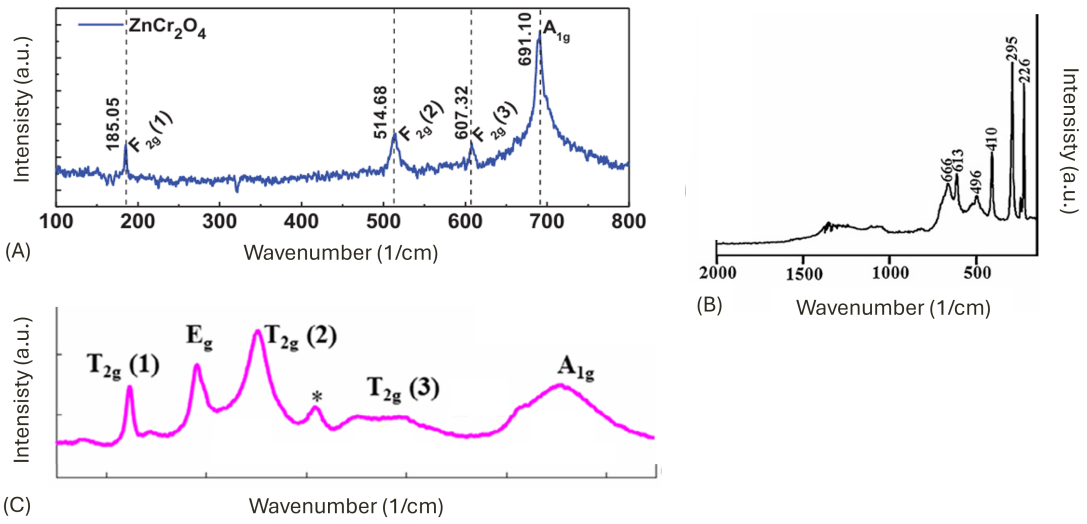

Figure 12: Raman spectra from literature. (A) $ZnCr_2O_4$ Raman spectra [41]. (B) $CuFe_2O_4$ Raman spectra [40]. (C) $ZnFe_2O_4$ Raman spectra, * unknown Raman band [11].

Figure 15, it is possible to state that the morphology of the nanoparticles is regular and they have an average size between 30 and 60 nm.

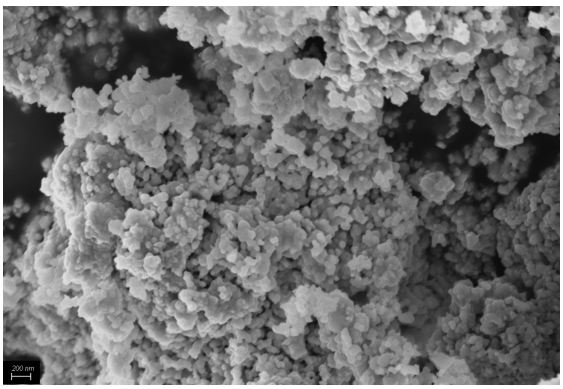

Figure 13: FESEM analysis of $ZnFe_2O_4$ nanoparticles with a magnification of 25.00KX. Scale bar is 200 nm.

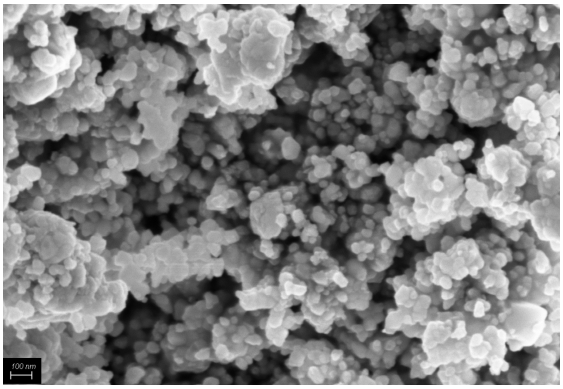

Figure 14: FESEM analysis of $CuFe_2O_4$ nanoparticles with a magnification of 50.00KX. Scale bar is 100 nm.

4.2 Cyclic voltammetry and Differential pulse voltammetry measurements

As previously explained in Section 3.6, the analyses were carried out through CV and DPV techniques. For each type of surface functionalization, CV analyses were useful to have a general idea of the process evolution. The Cyclophosphamide reduction process is detected by the formation of a small current peak in the bottom phase of the CV cycle; the same reaction, analysed through a DPV analysis, is characterized by a greater peak of the current, which is easier to identify and to study; an example of this behaviour is shown in Figure 16. Therefore, most of the

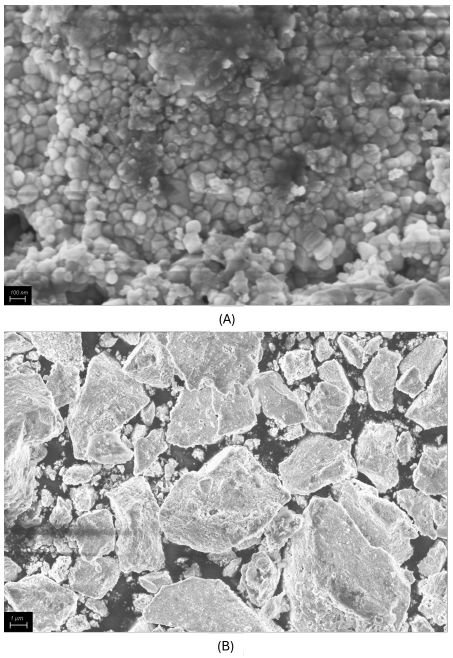

Figure 15: FESEM analysis. (A) $ZnCr_2O_4$ nanoparticles with a magnification of 50.00KX. Scale bar is 100 nm. (B) $ZnCr_2O_4$ nanoparticles with a magnification of 5.00KX. Scale bar is 1 µm.

considerations and conclusions reached in this work are based on the analysis of DPV results, which, in the study of Cyclophosphamide, provides more readable information than CV analysis.

It has been studied and demonstrated that Cyclophosphamide undergoes an irreversible reduction process inside the body thanks to the action of CYP P450 [18], [26]. However, especially with electrode surface functionalization with enzymes, in the upper part of the CV cycle, that is the oxidative region, there is a peak proportional to the increase in drug concentration, as shown in Figure 17: this phenomenon is unexpected since the drug undergoes only a reductive process, under physiological conditions. Moreover, this aspect is not highlighted in the DPV analysis. A possible hypothesis to explain the formation of this peak is that the drug is carrying out an oxidative, not physiological, process at the interface with the electrode surface, probably because the conditions reproduced in the analyses are not exactly comparable to the environment inside the body. Alternatively, the phenomenon could be attributed to an enzymatic oxidative process.

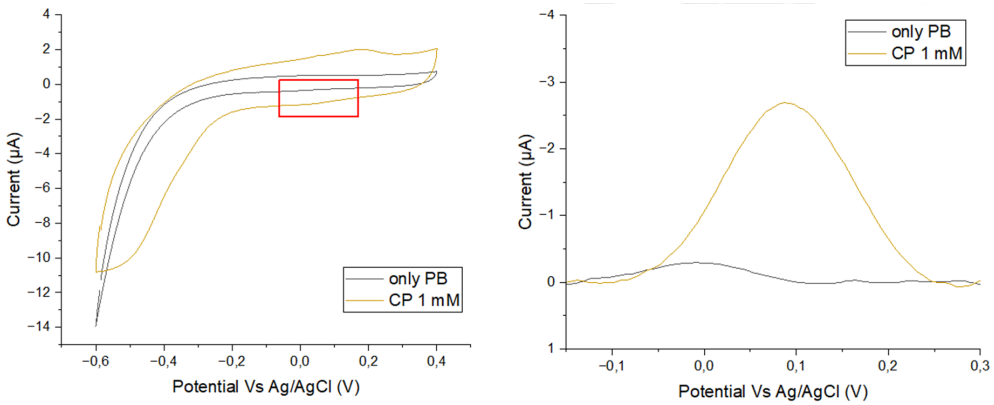

Figure 16: On the right: electrode with CYP P450 3A4, CV analysis. The red box highlights the reduction zone. On the left: electrode with CYP P450 3A4, DPV analysis with baseline subtraction.

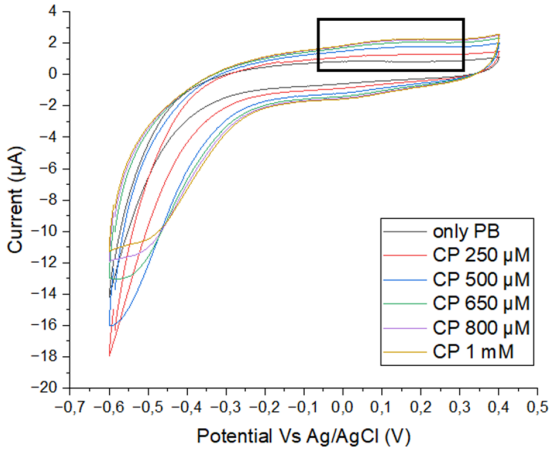

Figure 17: Electrode functionalized with $ZnCr_2O_4$ and CYP P450 2B6, CV analysis. The black box highlights the oxidation zone.

4.2.1 Surface functionalizations comparison

As shown in Table 7, different surface functionalizations have been tested, in order to develop the most complete comparisons. All the following figures represent the DPV analysis graphs subjected to baseline subtraction, to make the evaluation of the results easier and more readable. First, the results with bare electrode show the maximum of current peak, with CP 1 mM, with a value of 0.30 ± 0.17 µA and the corresponding potential is - 0.19 ± 0.02 V. Since the curve with only PB is almost flat, it can be deduced that the formation of the peak is due to the drug; however, there is no substantial difference between the results obtained with different concentrations of CP solution (Figure 18).

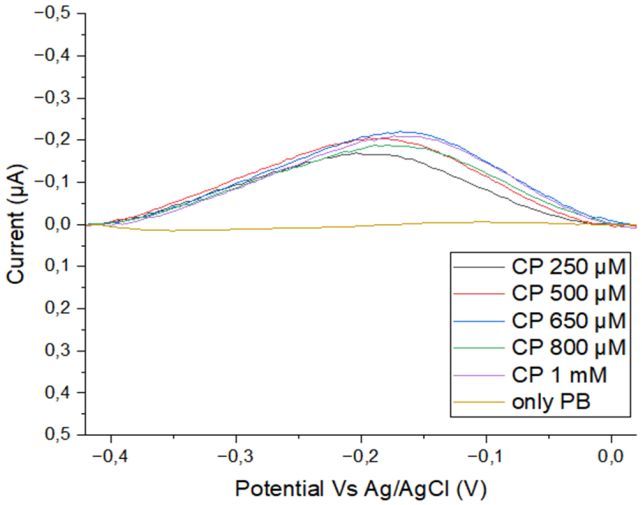

Figure 18: Bare electrode, DPV analysis (baseline subtraction).

Figure 19 shows the results in presence of $ZnCr_2O_4$, $ZnFe_2O_4$ and $CuFe_2O_4$ nanoparticles on the electrode surface. The maximum of current peak, with CP 1 mM, has a value on the order of hundreds of nA for all the three materials, that is comparable to the behaviour observed with bare electrode. Only the surface functionalization with $ZnCr_2O_4$ leads to a shift in the potential to the value of 0.07 ± 0.01 V: this material promotes the reduction of the drug more than the other two, reducing the energy needed to make the electronic exchange happen.
The presence of the enzymes alone leads to an increase in the maximum current peak by an order of magnitude, compared to the condition of the nanoparticles alone. Moreover, a clearer distinction can be observed between the different curves obtained with different concentrations of the drug.
As shown in Figure 20, CYP P450 3A4 performs better than CYP P450 2B6, with the maximum of current peak, with CP 1 mM, of 2.97 ± 0.40 µA, which corresponds to a potential of 0.08 ± 0.01 V. Instead, with the enzyme CYP P450 2B6, the maximum of current peak, with CP 1 mM, is 1.86 ± 0.34 µA, corresponding to a potential of - 0.15 ± 0.01 V. The presence of the peak in the test with only PB is due to a reaction involving the enzyme, as it is an organic molecule and it undergoes a redox process.
The best general results are obtained with the synergetic coupling of spinel oxides nanoparticles and CYPs: thanks to the simultaneous presence of biological and non-biological material is possible to obtain reductions peaks with higher values both compared to nanoparticles alone and to enzymes alone. Furthermore, hybrid functionalization makes the reductive process take place at higher potentials.

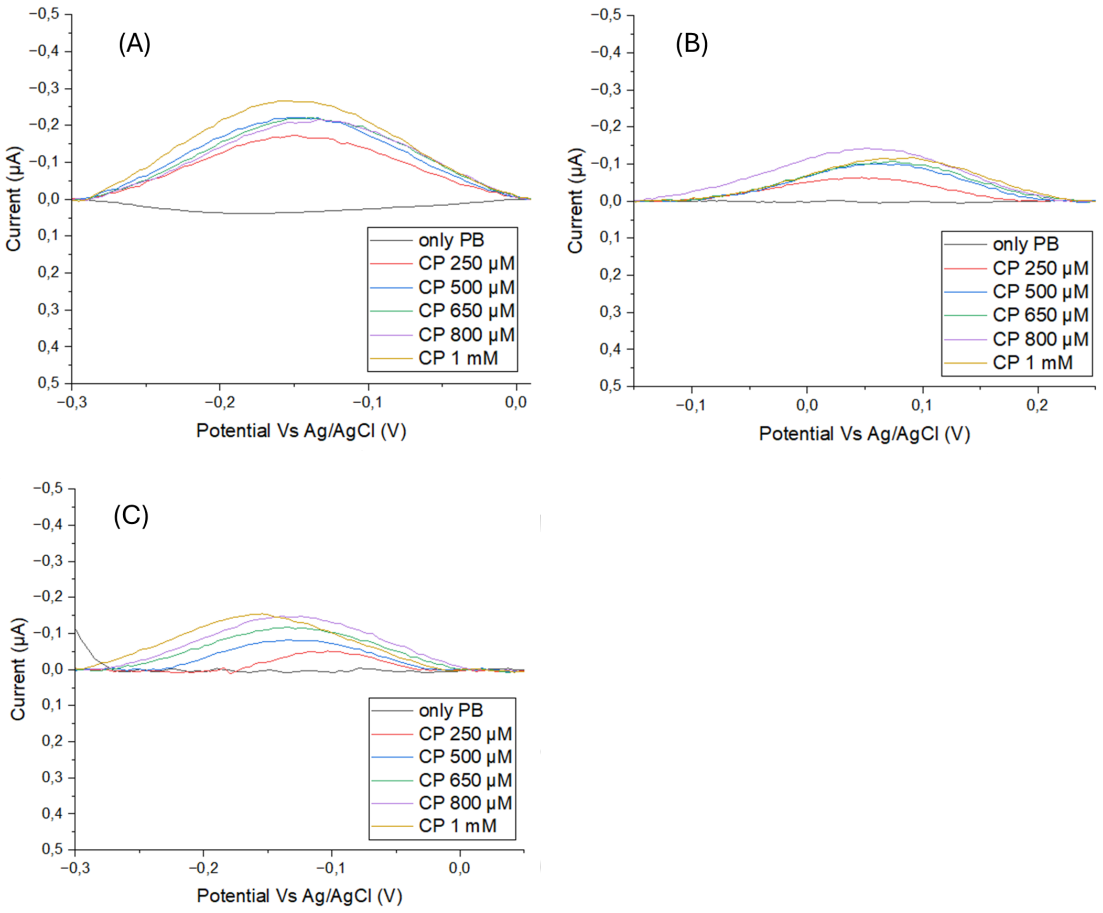

Figure 19: Surface functionalization with metal oxide nanoparticles, DPV analysis and baseline subtraction. (A) Electrode with $ZnFe_2O_4$. (B) Electrode with $ZnCr_2O_4$. (C) Electrode with $CuFe_2O_4$.

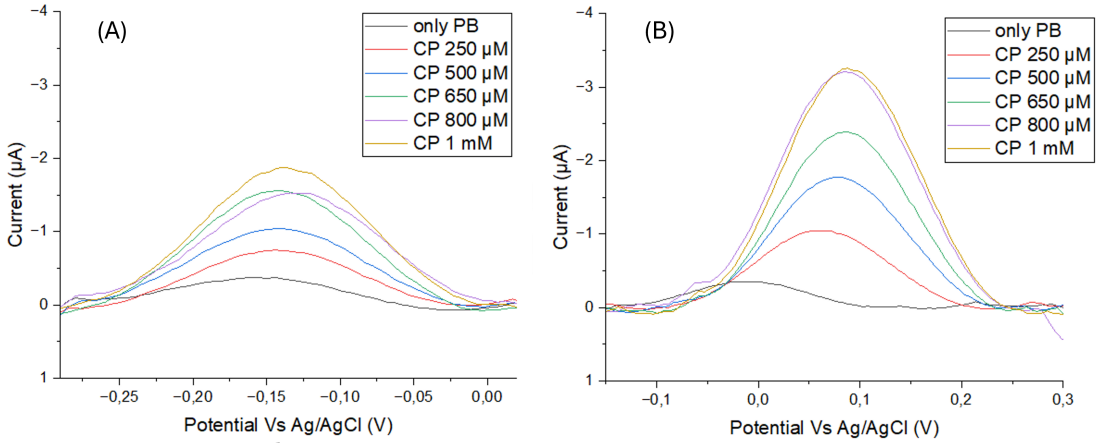

Figure 20: DPV analysis with baseline subtraction. (A) Electrode with CYP P450 2B6. (B) Electrode with CYP P450 3A4.

With nanoparticles and CYP P450 3A4 functionalization, the maximum of current peak, with CP 1 mM, is 4.50 ± 0.10 µA, 4.33 ± 0.43 µA and 5.64 ± 1.34 µA, respectively with zinc ferrite, zinc chromite e copper ferrite. These values are a few µA units higher than the condition of CYP P450 3A4 alone, while they are higher by an order of magnitude than the nanoparticles alone.
On the other hand, in the case of nanoparticles and CYP P450 2B6, the maximum of current peak, with CP 1 mM, is 8.15 ± 0.44 µA, 9.24 ± 0.65 µA and 9.64 ± 0.57 µA, respectively with zinc ferrite, zinc chromite e copper ferrite. This is the condition that guarantees the highest values of the current peak; in detail, the functionalization with $ZnCr_2O_4$ nanoparticles and CYP P450 2B6 leads to the highest enhanced signal (Table 8). The potential corresponding to the peak current has the value of 0.07 ± 0.01 V, in all these six conditions. Furthermore, as it can be seen in the Figure 21, the curves obtained with different drug concentrations are easily distinguishable and the peak value increases proportionally with the increase in the drug concentration: this phenomena will be explored in Section 4.3 through the calibration curves.

Functionalization	**Max of current peak (µA) CP 250 µM**	**Max of current peak (µA) CP 1 mM**	**Potential of peak (V)**
Bare electrode	0.25 ± 0.14	0.30 ± 0.17	- 0.19 ± 0.02
$ZnFe_2O_4$	0.12 ± 0.05	0.19 ± 0.07	- 0.15 ± 0.01
$ZnCr_2O_4$	0.05 ± 0.03	0.11 ± 0.03	0.07 ± 0.01
$CuFe_2O_4$	0.03 ± 0.03	0.11 ± 0.04	- 0.14 ± 0.02
CYP 2B6	0.86 ± 0.15	1.86 ± 0.34	- 0.15 ± 0.01
CYP 3A4	0.97 ± 0.11	2.97 ± 0.40	0.08 ± 0.01

Functionalization	**CYP 2B6**	**CYP 3A4**	**CYP 2B6**	**CYP 3A4**	**CYP 2B6**	**CYP 3A4**
$ZnFe_2O_4$	5.75 ± 0.19	2.06 ± 0.22	8.15 ± 0.44	4.50 ± 0.10	0.07 ± 0.01	0.07 ± 0.01
$ZnCr_2O_4$	4.81 ± 0.39	1.64 ± 0.09	9.24 ± 0.65	4.33 ± 0.43	0.07 ± 0.01	0.08 ± 0.01
$CuFe_2O_4$	6.09 ± 0.40	2.56 ± 0.87	9.64 ± 0.57	5.64 ± 1.34	0.06 ± 0.01	0.07 ± 0.01

Table 8: Summary of the results: maximum current peak CP 250 µM, maximum current peak CP 1 mM and potential of the peak corresponding to all the surface functionalizations exploited. The red values are the best performance.

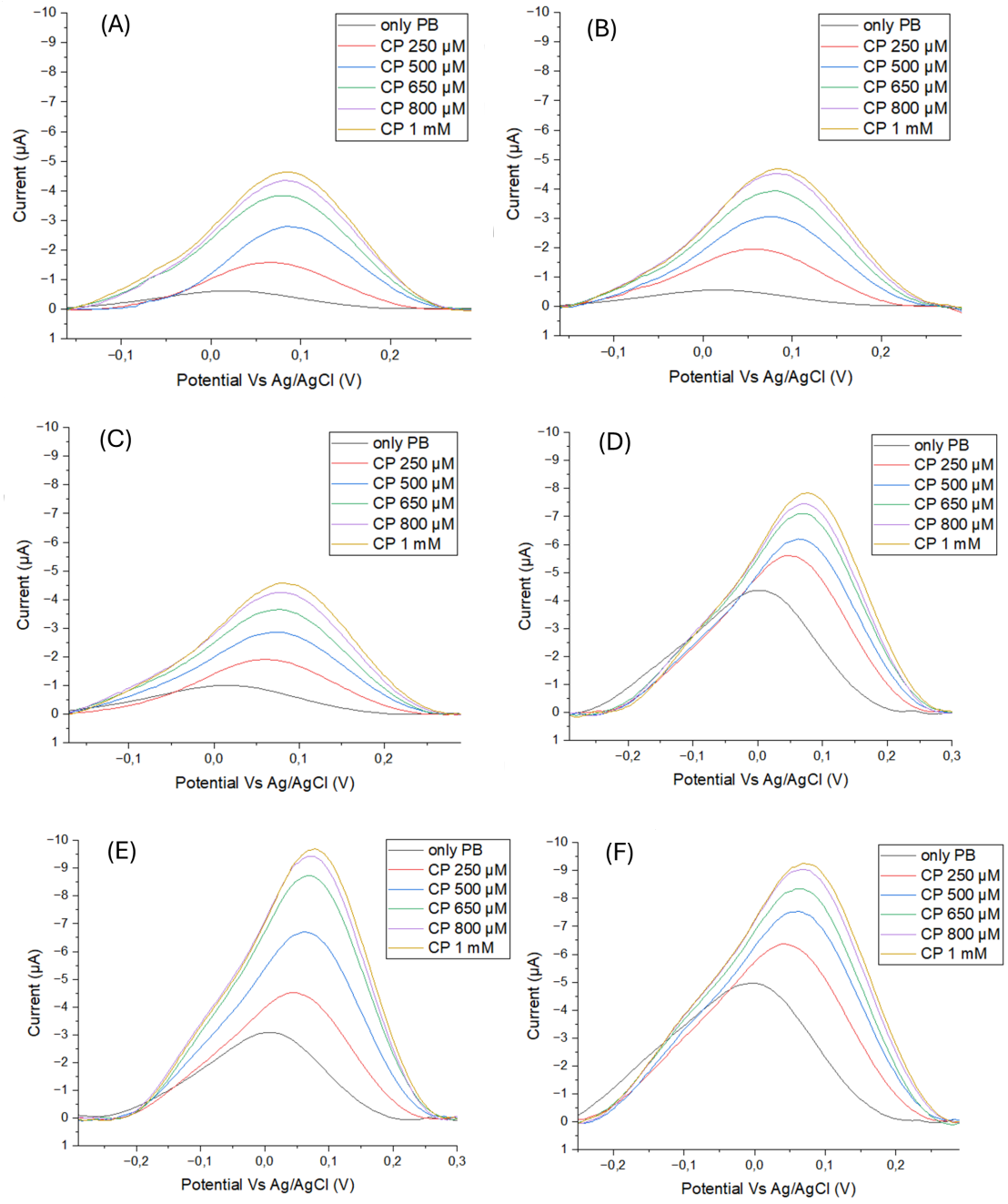

Figure 21: Hybrid surface functionalizations, DPV analysis with baseline subtraction. (A) Electrode with $ZnCr_2O_4$ and CYP P450 3A4. (B) Electrode with $CuFe_2O_4$ and CYP P450 3A4. (C) Electrode with $ZnFe_2O_4$ and CYP P450 3A4. (D) Electrode with $ZnFe_2O_4$ and CYP P450 2B6. (E) Electrode with $ZnCr_2O_4$ and CYP P450 2B6. (F) Electrode with $CuFe_2O_4$ and CYP P450 2B6.

The limit of detection is an additional parameter that characterize the performance of surface functionalization; in this work, the best performance is with $ZnFe_2O_4$ nanoparticles and CYP P450 3A4, with a value of 20.04 ± 0.98 µM (Table 9). The therapeutic range of use of the molecule under analysis is typically from 2 to 6 mg/kg body weight daily [42], which corresponds to a concentration range between 2.3 nM and 6.8 nM. This means that further studies and optimization processes are needed to better understand these hybrid surface functionalizations concerning the drug detection field.

Limit of detection (µM)		
Surface functionalization	**CYP P450 2B6**	**CYP P450 3A4**
$ZnCr_2O_4$ **NPs**	97.35 ± 5.33	25.61 ± 0.61
$ZnFe_2O_4$ **NPs**	101.31 ± 7.24	20.04 ± 0.98
$CuFe_2O_4$ **NPs**	339.89 ± 33.99	142.88 ± 9.53

Table 9: Limit of detection obtained through surface functionalization with $ZnCr_2O_4$, $ZnFe_2O_4$ and $CuFe_2O_4$ nanoparticles together with CYP P450 2B6 and CYP P450 3A4. The red value is the best performance.

The following figures show the average values of three electrodes obtained from the DPV analysis. The graphs were subjected to baseline subtraction and they also present the standard deviation. Figure 22 allows to highlight how much the presence of the enzyme guarantees an amplification of the detected signal; on the contrary, the behavior of the three metal oxides, shown in Figure 23, is comparable to the bare electrode. Finally, through Figure 24 and Figure 25, it is visually confirmed that hybrid surface functionalization leads to the best performance for the detection of Cyclophosphamide.

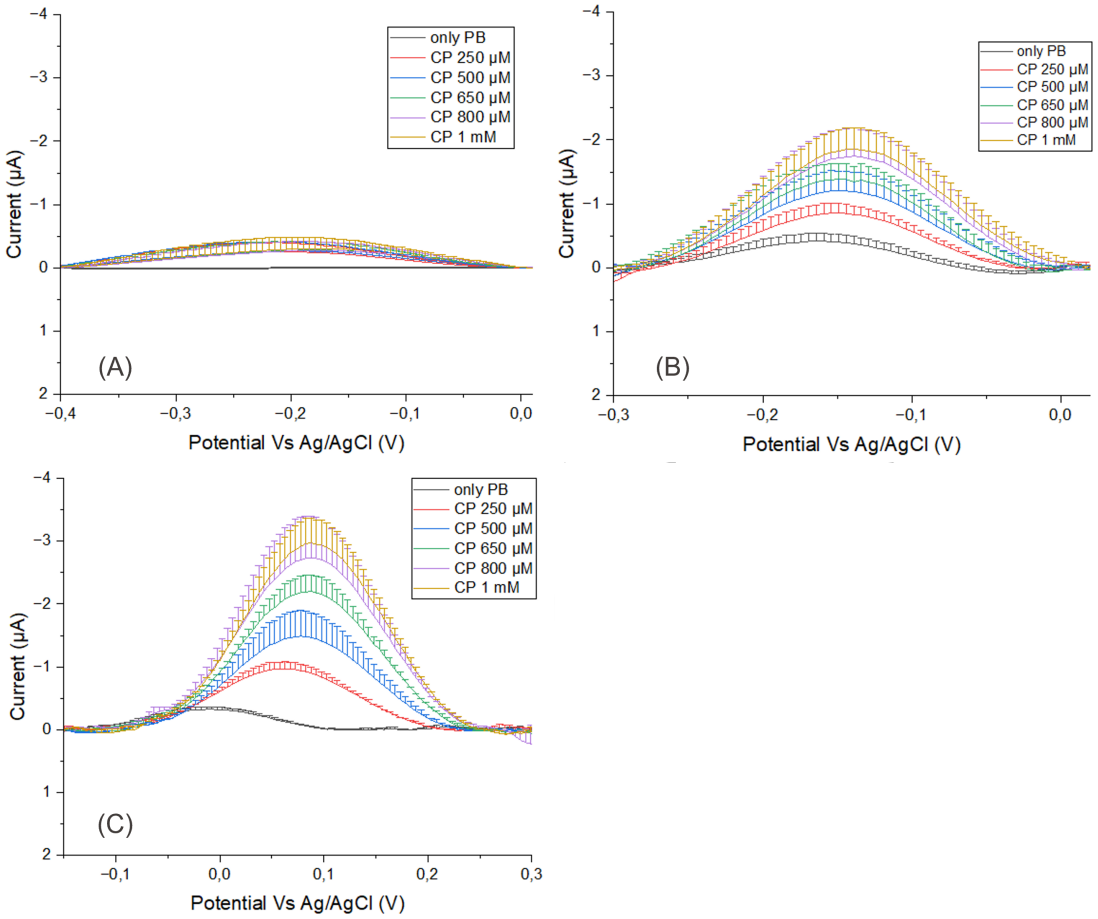

Figure 22: Average values of three electrodes, DPV analysis with baseline subtraction and standard deviation. (A) Bare electrode. (B) Electrode with CYP P450 2B6. (C) Electrode with CYP P450 3A4.

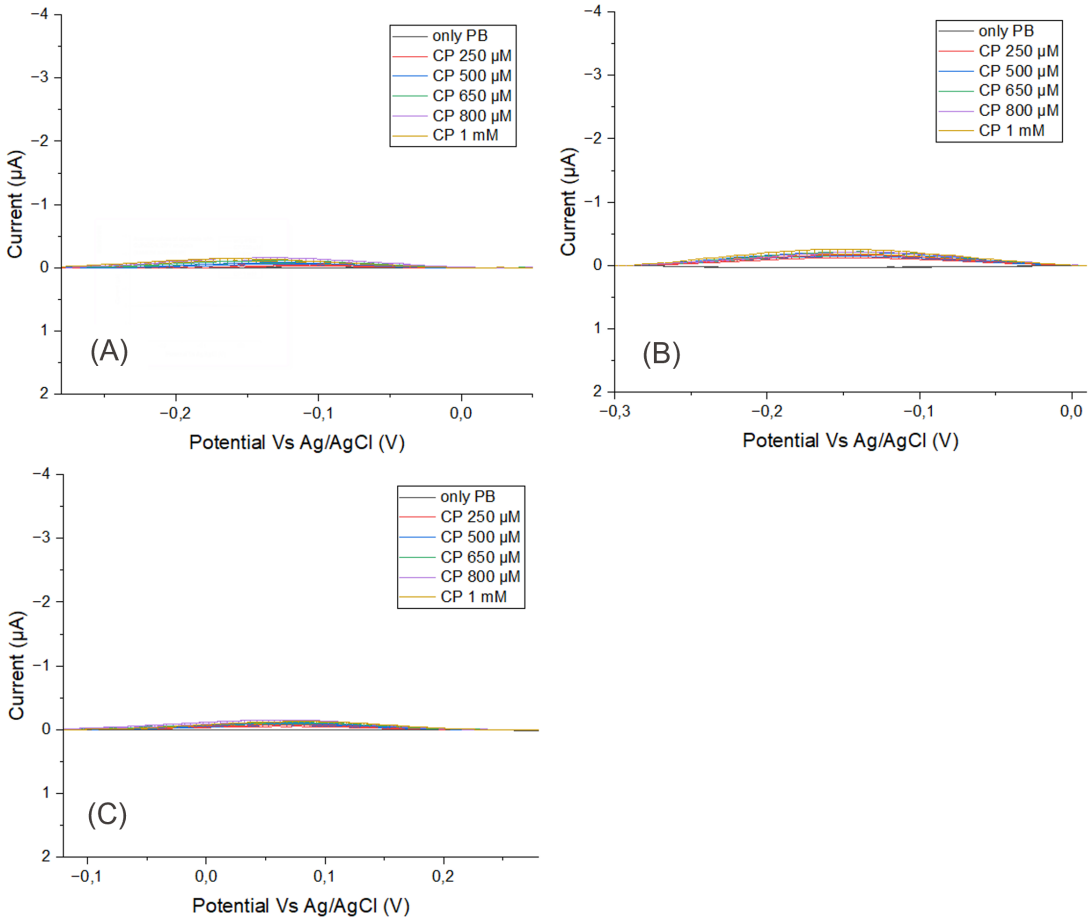

Figure 23: Average values of three electrodes, DPV analysis with baseline subtraction and standard deviation. (A) Electrode with $CuFe_2O_4$. (B) Electrode with $ZnFe_2O_4$. (C) Electrode with $ZnCr_2O_4$.

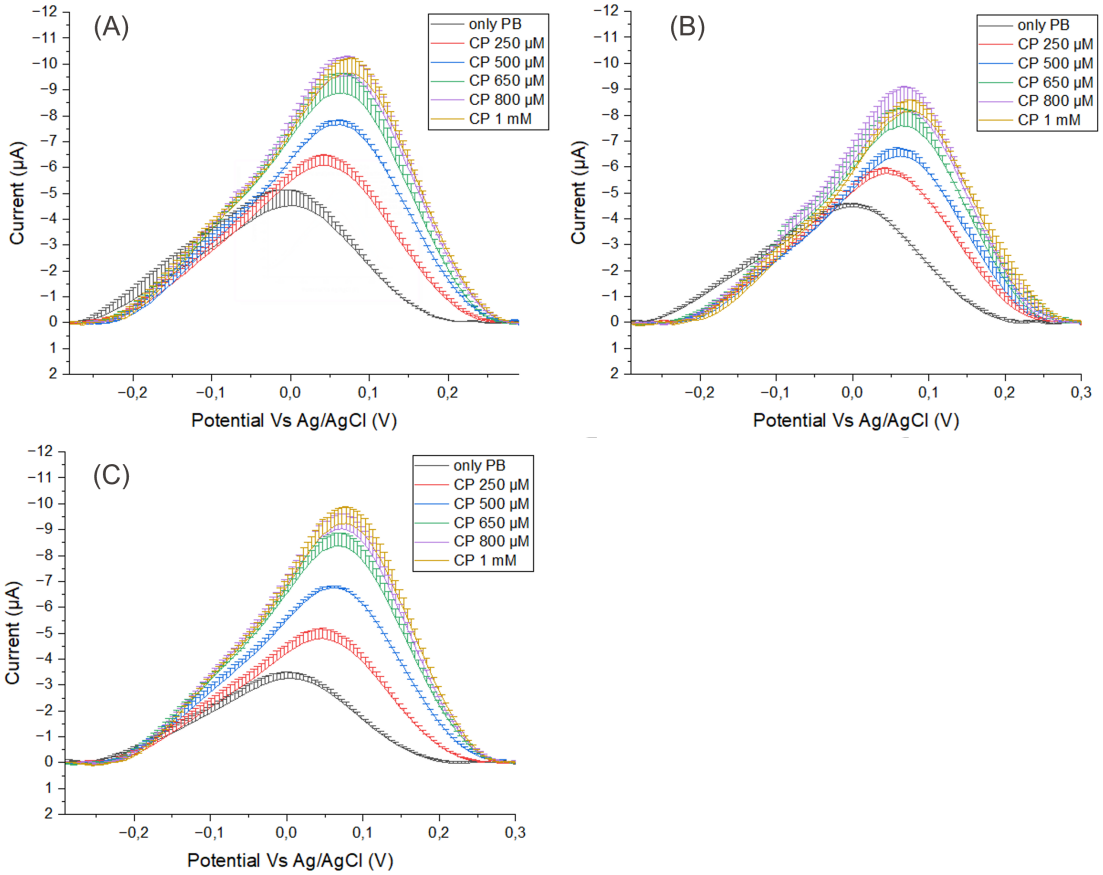

Figure 24: Average values of three electrodes, DPV analysis with baseline subtraction and standard deviation. (A) Electrode with $CuFe_2O_4$ and CYP P450 2B6. (B) Electrode with $ZnFe_2O_4$ and CYP P450 2B6. (C) Electrode with $ZnCr_2O_4$ and CYP P450 2B6.

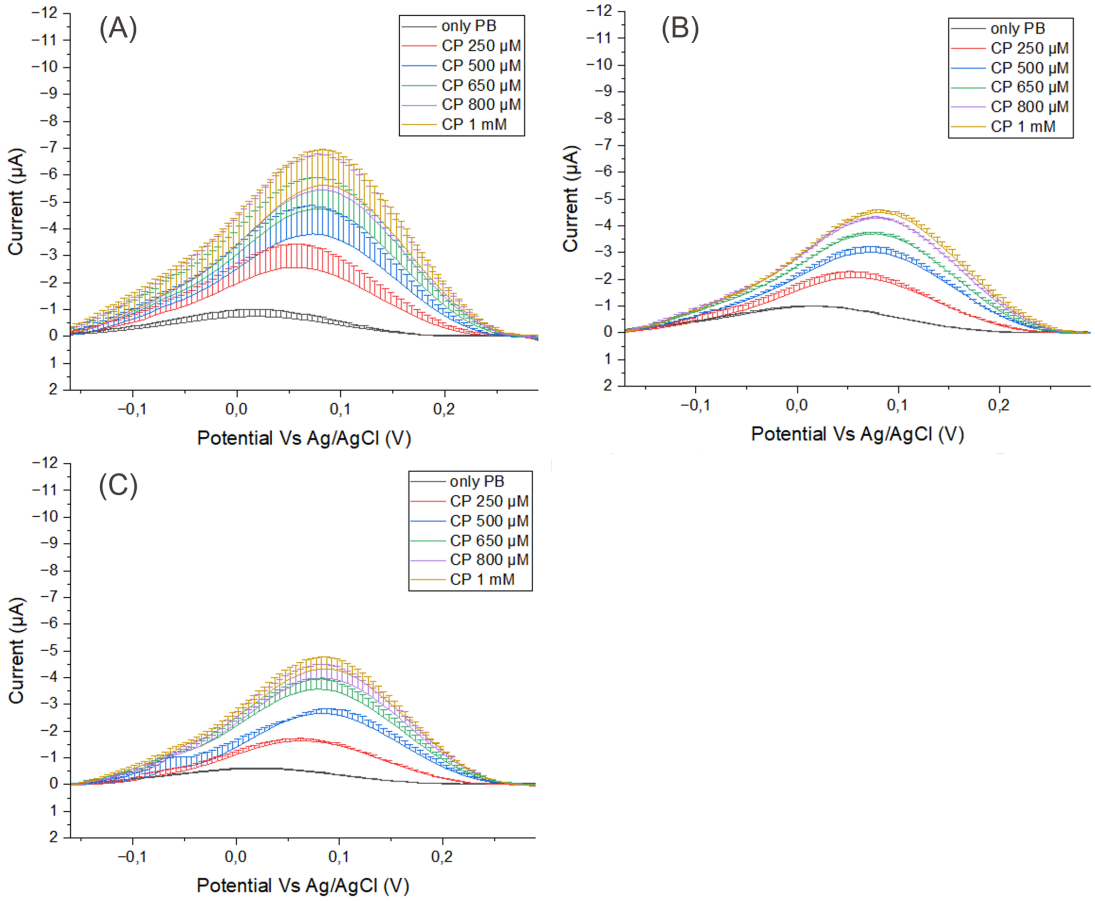

Figure 25: Average values of three electrodes, DPV analysis with baseline subtraction and standard deviation. (A) Electrode with $CuFe_2O_4$ and CYP P450 3A4. (B) Electrode with $ZnFe_2O_4$ and CYP P450 3A4. (C) Electrode with $ZnCr_2O_4$ and CYP P450 3A4.

4.3 Calibration curves

Figure 26 shows the calibration curves, where, for each concentration considered, the average value of the peak current on three electrodes and the relative standard deviation were reported.
Through the calibration curve slope, it is possible to derive the sensitivity granted by the different types of functionalizations.

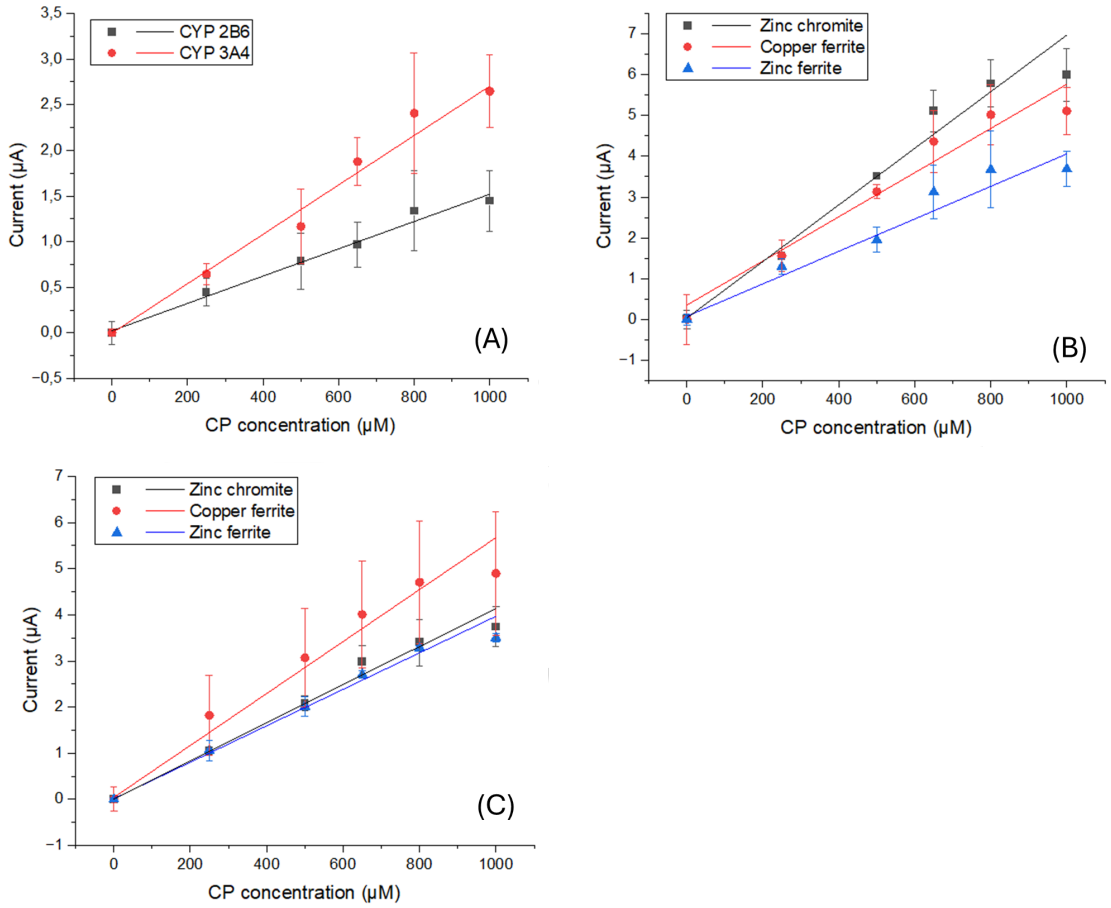

Figure 26: (A) Calibration curves of CYP P450 2B6 and CYP P450 3A4 functionalized electrodes. (B) Calibration curves of spinel oxides nanoparticles and CYP P450 2B6 functionalized electrodes. (C) Calibration curves of spinel oxides nanoparticles and CYP P450 3A4 functionalized electrodes.

As shown in Table 10, the sensitivity of bare electrode and electrode functionalized with nanoparticles alone is tens of pA/μM. The presence of the enzymes alone allows an increase in sensitivity of one order of magnitude: the functionalization with CYP P450 2B6 guarantees a sensitivity of 1.53 ± 0.50 nA/μM, while, with CYP P450 3A4, the sensitivity is 2.71 ± 0.09 nA/μM. Higher values of this characterizing parameter are observed with the hybrid functionalizations: the best

performance is in the case of $ZnCr_2O_4$ and CYP P450 2B6 with a value of 6.90 ± 0.41 nA/µM.

Functionalization	**Sensitivity (nA/µM)**	R^2
Bare electrode	0.06 ± 0.01	0.86
$ZnFe_2O_4$ **NPs**	0.09 ± 0.01	0.98
$ZnCr_2O_4$ **NPs**	0.09 ± 0.02	0.86
$CuFe_2O_4$ **NPs**	0.13 ± 0.02	0.91
CYP P450 2B6	1.53 ± 0.50	0.98
CYP P450 3A4	2.71 ± 0.09	0.99

Functionalization	**CYP 2B6**	**CYP 3A4**	**CYP 2B6**	**CYP 3A4**
$ZnFe_2O_4$ **NPs**	3.90 ± 0.32	3.9 ± 0.16	0.96	0.99
$ZnCr_2O_4$ **NPs**	6.90 ± 0.41	4.1 ± 0.13	0.98	0.99
$CuFe_2O_4$ **NPs**	5.4 ± 0.56	5.6 ± 0.36	0.95	0.97

Table 10: Sensitivity values corresponding to all the surface functionalizations exploited. The red value is the best performance.

Chapter 5

Conclusion

Nanostructured metal oxides, with spinel crystalline structure, are attractive for electroanalytical methodologies because they could improve the catalytic activity of the redox process of some molecules. The aim of this thesis project is to study the electrochemical behavior of zinc chromite, zinc ferrite and copper ferrite in relation to Cyclophosphamide in presence of CYPs P450 in his two isoforms of 3A4 or 2B6.

The nanoparticles, produced through autocombustion technique, were characterized morphologically and chemically through Field emission scanning electron microscopy and Raman spectroscopy. Spinel oxides nanoparticles and CYPs were then used to tailor the surface of screen-printed carbon electrodes by drop casting technique. The analyses were carried out with drug concentrations between 250 µM and 1 mM, using cyclic voltammetry and differential pulsed voltammetry techniques; the maximum peak of the current, the corresponding potential, the sensitivity of the detection and the limit of the detection were evaluated in different conditions.

The results of bare electrode and spinel nanomaterials functionalized electrodes are comparable, providing a maximum Faradic current peak of 0.18 ± 0.08 µA with a sensitivity of 0.09 ± 0.04 nA/µM, obtained by the linear calibration of the sensor. Surface functionalization only with enzymes leads to an increase in the maximum current peak and in the sensitivity by an order of magnitude. The best results are obtained with the synergetic coupling of nanostructured metal oxide and CYPs: in detail, the functionalization with zinc chromite nanoparticles and CYP P450 2B6 leads to a maximum of current peak of 9.24 ± 0.65 µA and a sensitivity of 6.90 ± 0.41 nA/µM. Instead, concerning the limit of detection, the best performance is with zinc ferrite nanoparticles and CYP P450 3A4, with a value of 20.04 ± 0.98 µM.

From the analyses carried out so far and presented in this work, it is possible to conclude that the presence of nanostructured oxides has a catalytic action on the reductive process of the CYPs, and consequently of the drug, enhancing the signal that is detected. Metal oxides with a normal spinel lattice with CYP P450 2B6 seem to guarantee the best performance for the detection of Cyclophosphamide.

This means that the presence of the Zn^{2+} cation in tetrahedral position, but above all, of the Fe^{3+} and Cr^{3+} cations in octahedral position in the crystalline lattice, have a catalyzing action on the redox process by interacting with the CYPs.
Promising results obtained suggest the necessity to conduct further research and investigations to optimize the application of these hybrid surface functionalizations in the field of biosensing. One aspect that can be improved is the synthesis process of metal powders to have a more standardized procedure, with greater uniformity and purity. In addition, the advantages and disadvantages that hybrid functionalization entails must be considered: the simultaneous presence of biological and non-biological components is essential to enhance the current signal. On one hand, it has been shown that the presence of nanoparticles alone does not lead to a significant amplification of the drug's reductive process. On the other hand, enzymes are sensitive molecules, which must be used in controlled environmental conditions to avoid their degradation. To make the most of the enzymatic activity, it is also necessary to optimize their surface immobilization process.
Metal oxide nanoparticles with a normal spinel crystallline structure guarantee the best performance: it is necessary to test other materials with the same characteristics to evaluate their electrochemical properties.
Finally, from a pharmaceutical point of view, only Cyclophosphamide has been tested, but spinel oxides could have a catalyzing action on other anticancer drugs as well. Moreover, it is essential to identify the most suitable organic molecule that facilitates and improves the interaction between the analyte and the electrode surface.

Bibliography

[1] Heru Saputra. "Electrochemical sensors: basic principles, engineering, and state of the art". In: *Monatshefte fuer Chemie/Chemical Monthly* 154 (Aug. 2023), p. 3.

[2] Kevin Beaver, Ashwini Dantanarayana, and Shelley Minteer. "Materials Approaches for Improving Electrochemical Sensor Performance". In: *The Journal of Physical Chemistry B* 125 (Oct. 2021).

[3] Fang Wei et al. "Electrochemical sensor for multiplex biomarkers detection". In: *Clinical Cancer Research* 15.13 (2009), pp. 4446–4452.

[4] R.A.S. Couto, J.L.F.C. Lima, and M.B. Quinaz. "Recent developments, characteristics and potential applications of screen-printed electrodes in pharmaceutical and biological analysis". In: *Talanta* 146 (2016), pp. 801–814. ISSN: 0039-9140.

[5] Metrohm. *Elettrodo a membrana in carbonio (Aus.:C; Rif.:Ag/AgCl) 11L*. Catalogue available on line. 2023.

[6] Bambang Kuswandi et al. "Water monitoring using polymer inclusion membranes: a review". In: *Environmental Chemistry Letters* 18 (2020), pp. 129–150.

[7] Mutasem Razem et al. "Analysis of Phenolic Compounds in Food by Coulometric Array Detector: A Review". In: *Sensors* 22.19 (2022).

[8] Sandro Carrara et al. "Multi-panel drugs detection in human serum for personalized therapy". In: *Biosensors and Bioelectronics* 26.9 (2011), pp. 3914–3919. ISSN: 0956-5663.

[9] Charaf Laghlimi et al. "Recent advances in electrochemical sensors and biosensors for monitoring drugs and metabolites in pharmaceutical and biological samples". In: 11 (June 2023), pp. 151–173.

[10] Rajalakshmi Sakthivel et al. "A Sandwich-Type Electrochemical Immunosensor for Insulin Detection Based on Au-Adhered Cu5Zn8 Hollow Porous Carbon Nanocubes and AuNP Deposited Nitrogen-Doped Holey Graphene". In: *Small* 18.35 (2022), p. 2202516.

[11] Mallikarjun Madagalam et al. “Unraveling the Effect of the Chemical and Structural Composition of Zn Ni1 Fe2O4 on the Electron Transfer at the Electrochemical Interface”. In: *Small Structures* 4.12 (2023), p. 2300163.

[12] Tetiana Tatarchuk et al. “Catalytic and Photocatalytic Properties of Oxide Spinels”. In: *Handbook of Ecomaterials*. Ed. by Leticia Myriam Torres Martínez, Oxana Vasilievna Kharissova, and Boris Ildusovich Kharisov. Cham: Springer International Publishing, 2018, pp. 1–50.

[13] D. Hernández-Ramírez et al. “Review—Trends on the Development of Non-Enzymatic Electrochemical Sensors Modified with Metal-Oxide Nanostructures for the Quantification of Uric Acid”. In: *Journal of The Electrochemical Society* 168.5 (June 2021), p. 057522.

[14] Yanchun Zhang, Chuanjin Yuan, and Aimin Sun. “Structural, magnetic, and optical properties of Al3+ ion-substituted Ni–Ba–Co ferrite prepared via sol–gel method”. In: *Journal of Materials Science: Materials in Electronics* 33.19 (June 2022), pp. 15495–15508.

[15] Zahrah Alhalili. “Metal Oxides Nanoparticles: General Structural Description, Chemical, Physical, and Biological Synthesis Methods, Role in Pesticides and Heavy Metal Removal through Wastewater Treatment”. In: *Molecules* 28.7 (2023). ISSN: 1420-3049.

[16] Thomas Girardet et al. “Spinel Magnetic Iron Oxide Nanoparticles: Properties, Synthesis and Washing Methods”. In: *Applied Sciences* 12.16 (2022). ISSN: 2076-3417.

[17] The Editors of Encyclopaedia. Britannica. *Enzyme definition and features*. Available on line. 22 Jul. 2024.

[18] Camilla Baj-Rossi, Giovanni De Micheli, and Sandro Carrara. *P450-based nano-bio-sensors for personalized medicine*. Vol. 21. Chapter, 2011.

[19] Ming Chen et al. “How do enzymes ‘meet’nanoparticles and nanomaterials?” In: *Trends in biochemical sciences* 42.11 (2017), pp. 914–930.

[20] Dayana Soto and Jahir Orozco. “Hybrid Nanobioengineered Nanomaterial-Based Electrochemical Biosensors”. In: *Molecules* 27.12 (2022). ISSN: 1420-3049.

[21] Orozco Jahir Cajigas Sebastian Alzate Daniel. “Gold nanoparticle/DNA-based nanobioconjugate for electrochemical detection”. In: *Mikrochim Acta* 187.11 (2020). ISSN: 1436-5073.

[22] Atieh Bahrami et al. “Covalent immobilization of cytochrome P450 BM3 (R966D/W1046S) on glutaraldehyde activated SPIONs”. In: *The Canadian Journal of Chemical Engineering* 96.10 (2018), pp. 2227–2235.

[23] Sandro Carrara et al. “Multi-panel drugs detection in human serum for personalized therapy”. In: *Biosensors and Bioelectronics* 26.9 (2011), pp. 3914–3919.

[24] Ana-Maria Chiorcea-Paquim and Ana Maria Oliveira-Brett. “Electrochemistry of chemotherapeutic alkylating agents and their interaction with DNA”. In: *Journal of Pharmaceutical and Biomedical Analysis* 222 (2023), p. 115036. ISSN: 0731-7085.

[25] The International Waldenstrom’s Macroglobulinemia Foundation. *Scheda informativa ciclofosfamide*. Febbraio 2021.

[26] PRIYANKA Sinha, SACHIN Doi, and DK Sharma. “Electrochemical Behaviour and Adsorptive Stripping Voltammetric Determination of Cyclophosphamide”. In: *Chem. Sci. Trans* 7.2 (2018), pp. 229–239.

[27] Thulfeqar Ahmed Hamza et al. “Cyclophosphamide drug sensing characteristics by using pure and Ti-doped graphyne-like BN-yne”. In: *Inorganic Chemistry Communications* 150 (2023), p. 110535. ISSN: 1387-7003.

[28] Sachin Doi Priyanka Sinha and D. K. Sharma. “Electrochemical Behaviour and Adsorptive Stripping Voltammetric Determination of Cyclophosphamide”. In: *Chemical Science Transactions* 7 (2018), pp. 229–239. ISSN: 2278-3458.

[29] Noémie Elgrishi et al. “A practical beginner’s guide to cyclic voltammetry”. In: *Journal of chemical education* 95.2 (2018), pp. 197–206.

[30] Elena Ghibaudi, Alberto Regis, and Ezio Roletto. “Le reazioni redox: un pasticcio concettuale?” In: *Perspectives in Science* 5 (2015). SI Progress in Science Education 2015, pp. 14–24. ISSN: 2213-0209.

[31] Breno Nascimento Ciribelli, Flavio Colmati, and Elki Cristina de Souza. “Nernst equation applied to electrochemical systems and centenary of his Nobel Prize in chemistry”. In: *International Journal for Innovation Education and Research* 8.11 (Nov. 2020), pp. 670–683.

[32] Henry S. White Allen J. Bard Larry R. Faulkner. *Electrochemical Methods: Fundamentals and Applications*. Wiley. ISBN: 978-0-471-04372-0.

[33] B. Jill Venton and Dana J. DiScenza. “Chapter 3 - Voltammetry”. In: *Electrochemistry for Bioanalysis*. Ed. by Bhavik Patel. Elsevier, 2020, pp. 27–50. ISBN: 978-0-12-821203-5.

[34] James L. Melville and Richard G. Compton. “The Simulation of Differential Pulse Voltammetry”. In: *Electroanalysis* 13.2 (2001), pp. 123–130.

[35] S. Mitchell J. Mocak A. M. Bond and G. Scollary. “Statistical overview of standard (IUPAC and ACS) and new procedures for determining the limits of detection and quantification: Application to voltammetric and stripping techniques (Technical Report)”. In: *Pure Appl. Chem.* 69 (1997), pp. 297–328.

[36] Hans-Peter Loock and Peter D. Wentzell. “Detection limits of chemical sensors: Applications and misapplications”. In: *Sensors and Actuators B: Chemical* 173 (2012), pp. 157–163. ISSN: 0925-4005.

[37] Gurvinder Singh Bumbrah and Rakesh Mohan Sharma. “Raman spectroscopy–Basic principle, instrumentation and selected applications for the characterization of drugs of abuse”. In: *Egyptian Journal of Forensic Sciences* 6.3 (2016), pp. 209–215.

[38] Anwar Ul-Hamid. “A Beginners’ Guide to Scanning Electron Microscopy”. In: (2018).

[39] Mallikarjun Madagalam et al. “Bismuth-Nanocomposites Modified SPCEs for Non-Enzymatic Electrochemical Sensors”. In: *IEEE Sensors Journal* 21.9 (2021), pp. 11155–11162.

[40] M Balaji, P Chithra Lekha, and D Pathinettam Padiyan. “Core–shell structure in copper ferrite–polyaniline nanocomposite: confirmation by laser Raman spectra”. In: *Vibrational Spectroscopy* 62 (2012), pp. 92–97.

[41] Pankaj Choudhary, Anand Yadav, and Dinesh Varshney. “Structural and optical studies of nanocrystalline ZnCr2O4 and CoCr2O4 spinel”. In: *AIP Conference Proceedings* 1832.1 (May 2017), p. 050051. ISSN: 0094-243X.

[42] S.D. Russell. “Chapter 26 - The Effects of Immunosuppressive and Cytotoxic Drugs on the Heart”. In: *The Heart in Rheumatic, Autoimmune and Inflammatory Diseases*. Ed. by Udi Nussinovitch. Academic Press, 2017, pp. 645–657. ISBN: 978-0-12-803267-1.

Acknowledgement

Ci tengo a ringraziare i Professori Sandro Carrara e Alberto Tagliaferro per avermi dato la possibilità di studiare presso i laboratori dell'EPFL a Neuchâtel e del Carbon Group al Politecnico di Torino.
Ringrazio Mattia Bartoli, Francesca Rodino e Mallikarjun Madagalam per avermi aiutato con i vostri consigli e la vostra esperienza durante tutto lo sviluppo del progetto di tesi.
Infine, ringrazio la mia famiglia, Daniele e i miei amici per l'affetto e il supporto durante questi cinque anni universitari, siete molto importanti per me.

I would like to thank Professors Sandro Carrara and Alberto Tagliaferro for giving me the opportunity to study at EPFL laboratories in Neuchâtel and in the Carbon Group at Politecnico di Torino.
I thank Mattia Bartoli, Francesca Rodino and Mallikarjun Madagalam for helping me with your advice and experience throughout the development of the thesis project.
Finally, I thank my family, Daniele and my friends for their affection and support during these five university years, you are very important to me.